PREPARATION AND CHARACTERIZATION OF ALUMINA LOADED TITANIA IN THE PHOTOREDUCTION OF CO_2

NORHASZJANA BINTI AWANG HASAN

UNIVERSITI MALAYSIA PAHANG

PREPARATION AND CHARACTERIZATION OF ALUMINA LOADED TITANIA IN THE PHOTOREDUCTION OF CO_2

NORHASZJANA BINTI AWANG HASAN

Thesis is submitted in fulfillment of the requirements for the award
of Bachelor of Chemical Engineering (Gas Technology)

Faculty of Chemical Engineering and Natural Resources
UNIVERSITI MALAYSIA PAHANG

JANUARY 2012

SUPERVISORS'S DECLARATION

I hereby declare that I have checked this thesis and in my opinion, this thesis is adequate in terms of scope and quality for the award of Bachelor of Chemical Engineering (Gas Technology).

Signature : .....

Name of Supervisor : Nor Khonisah Binti Daud

Position :

Date :

STUDENT'S DECLARATION

I declare that this thesis entitled "Preparation and Characterization of Alumina loaded Titania in the photoreduction of CO_2" is the result of my own research except as cited in the references. The thesis has not been accepted for any degree and is not concurrently submitted in candidature of any other degree.

Signature : .....

Name : Norhaszjana Binti Awang Hasan

ID Number : KC08042

Date :

Special dedication to my family

Especially to my supportive parents;

Awang Hasan Bin Awang Hashim and Aishah Abdullah

Not-so-my siblings

My supervisor

Miss Nor Khonisah Binti Daud

and

all my friends

For all your endless love, support and encouragement towards me.

ACKNOWLEDGEMENTS

First of all, I thank Almighty Allah who blessed me and made it possible for me to complete my Undergraduate Research Project. Special thanks to my supervisor, Miss Nor Khonisah Binti Daud for her cooperation and willingness in sharing ideas, knowledge and guidance during the research. The supervision and support that she gave truly help the progression and smoothness of the research. The co-operation is much indeed appreciated.

Great deals appreciated go to the contribution of Faculty of Chemical Engineering and Natural Resources (FKKSA) staffs especially all the assistant vocational training officer for their kind assistance and cooperation in handling the equipment in the laboratory and in purchasing the chemicals needed for my research. Other than that, I also owe my most sincere gratitude to Faculty of Industrial Sciences and Technology (FIST), Mr Shaharudin and Central Laboratory assistant lab, for their willingness to help me in analyzing the samples for my research.

Last but not least, I would like to express my token of appreciation to my wonderful family for their unconditional support, motivation and care towards this research. Not forget, great appreciations go to my friends who had helped me from time to time during the research. Infinite gratitude to all as I could not mention all names in this limited space.

ABSTRACT

Nowadays, the atmospheric concentration of carbon dioxide (CO_2) had been increased due to the globalization and technology created by human activities. CO_2 is one of the major contributors to greenhouse effects which will leads to global warming. Therefore alternative routes should be taken to overcome this problem. One of the best remediation is to transform CO_2 into useful hydrocarbon by using photoreduction. Photoreduction is one of the methods which can be used to reduce the concentration of CO_2 released to the atmosphere. The aim of this study was to find a new catalyst produced with the best method in photoreduction process. Catalyst plays an important role to accomplish specific tasks with greater efficiency and speed. The metal oxides, Alumina (Al_2O_3) was chosen to be use in this research which was loaded with Titania (TiO_2). Al_2O_3-TiO_2 catalyst was prepared by using two different methods which are sol gel and hydrothermal method. The prepared catalysts were analyzed and characterized by using Scanning Electron Microscope (SEM), Fourier Transform Infrared Spectroscopy (FTIR), X-Ray diffraction (XRD) and Brunauer-Emmett-Teller (BET) method. Experimental results demonstrated that hydrothermal method was a promising technique for preparing Al_2O_3-TiO_2 photocatalysts as it fulfilled the requirement properties to enhance the photocatalytic activity of TiO_2 in the photoreduction process. Based on SEM analysis, the surface morphology of Al_2O_3-TiO_2 catalyst exhibits well arranged aggregates with many small spherical particles. Meanwhile FTIR analysis, the presence of Al-O bonds in the TiO_2 powder was successfully obtained as the peaks of 947.75 cm^{-1} fall in the general range of Al-O vibrations. Other than that, based on XRD pattern of Al_2O_3-TiO_2 it revealed the existence of polymorphs anatase TiO_2 which usually shows greatly superior in photoactivity of TiO_2. Most importantly, based on BET analysis, the prepared Al_2O_3-TiO_2 catalysts show a great crystal growth with 153.8599 m^2/g specific surface area and 8.8 nm of pore size diameter. A nano size material leads to improvement in the electron hole pair separation and enhance the photoactivity of TiO_2.

ABSTRAK

Pada masa kini, jumlah kepekatan karbon dioksida (CO_2) di dalam udara telah meningkat disebabkan oleh globalisasi dan teknologi yang dicipta oleh aktiviti manusia. CO_2 adalah salah satu penyumbang utama kepada kesan rumah hijau yang akan membawa kepada pemanasan global. Oleh itu, langkah alternatif harus diambil untuk mengatasi masalah tersebut. Salah satu kaedah yang terbaik untuk menjadikan CO_2 kepada jenis hidrokarbon yang berguna dengan menggunakan kaedah photoreduksi. Photoreduksi adalah salah satu kaedah yang boleh digunakan untuk mengurangkan kadar kepekatan CO_2 yang dilepaskan ke atmosfera. Tujuan kajian ini adalah untuk mencari mangkin baru yang akan dihasilkan dengan kaedah yang terbaik dalam proses photoreduksi. Mangkin memainkan peranan yang penting untuk menyempurnakan tugas-tugas tertentu dengan lebih berkesan dan pantas. Oksida logam, Alumina (Al_2O_3) telah dipilih untuk digunakan dalam penyelidikan ini yang akan dicampur dengan Titania (TiO_2). Mangkin Al_2O_3-TiO_2 telah disediakan dengan menggunakan dua kaedah yang berbeza iaitu kaedah sol gel dan kaedah hidroterma. Mangkin yang telah disediakan, dianalisa dan dicirikan dengan menggunakan Mikroskop Elektron Imbasan (SEM), Spektroskopi Fourier Transform Infrared (FTIR), pembelauan X-Ray (XRD) dan kaedah Brunauer-Emmett-Tellar (BET). Keputusan uji kaji menunjukkan bahawa kaedah hidroterma adalah satu teknik yang bagus untuk menyediakan mangkin Al_2O_3-TiO_2 kerana ia memenuhi ciri-ciri untuk meningkatkan kadar aktiviti photobermangkina TiO_2 dalam proses photoreduksi. Berdasarkan analisis SEM, morfologi permukaan mangkin Al_2O_3-TiO_2 mempamerkan agregat yang disusun dengan banyak zarah sfera kecil. Sementara itu, analisa FTIR, membuktikan bahawa kehadiran ikatan Al-O dalam mangkin TiO_2 telah berjaya diperolehi iaitu pada puncak 947.75 cm^{-1} yang jatuh dalam julat am getaran ikatan Al-O. Selain daripada itu, berdasarkan corak XRD Al_2O_3-TiO_2, ia mendedahkan kewujudan fasa anatase zarah TiO_2 yang biasanya menunjukkan banyak manfaat dalam photoaktiviti TiO_2. Paling penting, berdasarkan analisa BET, mangkin Al_2O_3-TiO_2 yang

disediakan menunjukkan pertumbuhan kristal yang hebat yang mempunyai 153.8599 m^2 / g permukaan kawasan tertentu dan saiz diameter liang zarah sebanyak 8.8 nm. Bahan saiz nano membawa kepada peningkatan dalam lubang pemisahan pasangan elektron dan akan meningkatkan kadar photoaktiviti TiO_2.

TABLE OF CONTENTS

CHAPTER 5 CONCLUSION AND RECOMMENDATIONS

LIST OF TABLES

LIST OF FIGURES

LIST OF SYMBOLS

^{o}	degree
^{o} C	degree celcius
Å	Amstrong
atm	atmospheric
cm^{-1}	per centi meter
cm^3/g	centimetre cube per gram
e^-	Negative electron
eV	Electron volt
g	gram
g/cm^3	gram per centimetre cube
h	hour
h^+	Positive electron
kV	kilo Volt
M	Molarity
mA	mili ampere
min	minute
mL	mili litre
m^2/g	meter square per gram
m/m-K	Thermal Expansion
nm	nanometer
rpm	Revolutions per minute
s	second
V	Voltage
W	Watt
W/m-K	Thermal Conductivity
X	Magnificent
μm	micro meter
λ	wavelength

LIST OF ABBREVIATIONS

Ag	Silver
ALCOA	Aluminum Company of America
Al_2O_3	Aluminium Oxide / Alumina
Al_2O_3-TiO_2	Alumina Titania
$Al(OC_3H_7)_3$	Aluminium isopropoxide
Ar	Argon
Au	Gold
B	Boron
BET	Brunauer-Emmett-Tellar
C	Carbon
CO_2	Carbon dioxide
cph	Closed packed hexagonal
cps	Counts per second
CVD	Vapour deposition
Fe	Iron
FTIR	Fourier Transform Infrared Spectroscopy
H	Hydrogen
$HAuCl_4.4H_2O$	Tetrachloroauric acid
HNO_3	Nitric acid
H_2O	Water
H_2O_2	Hydrogen peroxide
H_2SO_4	Sulphuric acid
IEA	International Energy Agency
IEP	Isoelectric points
IPCC	Intergovernmental panel on climate change
IR	Infrared intensity
N	Nitrogen
NH_3	Ammonia
NO	Nitrogen oxides
OH	Hydroxide
O_2	Oxygen
P	Phosphorus
ppmv	Parts per million in volume
Pt	Platinum
PVD	Physical vapour deposition
S	Sulfur
SEM	Scanning Electron Microscope
SiO_2	Silica
ST	Standard Titania powder
TBOT	Titanium tetrabutoxide
Ti	Titanium
$TiCl_4$	Titanium tetrachloride
TiN	Titanium nitride
TiO_2	Titanium dioxide / Titania
$Ti(OBu)_4$	Titanium Butoxide
$Ti(OC_3H_7)_4$	Titanium-tetra-isopropoxide

TIP	Titanium phosphide
TiS_2	Titanium disulfide
$Ti(SO_4)_2$	Titanium sulfate
V	Vanadium
XRD	X-Ray diffraction

CHAPTER 1

INTRODUCTION

1.1 Background study

Carbon dioxide (CO_2) is one of the green house gases which cause the global warming. According to International Energy Agency (IEA) (2011), the atmospheric concentration of CO_2 has recently increased about 280 parts per million in volume (ppmv) due to the globalization and technology created by human activities.

Some impacts of the increased of CO_2 emissions concentrations may be slow to become apparent since stability is an inherent characteristic of the interacting climate, ecological and socio-economic systems. Besides that, even after stabilisation of the atmospheric concentration of CO_2, anthropogenic warming and sea level rise are still would continue for centuries due to the time scales associated with climate processes and feedbacks (IPCC, 2007). Some changes in the climate system would be irreversible in the course of a human lifespan.

Moreover, due to the long lifetime of CO_2 in the atmosphere, stabilising concentrations of greenhouse gases at any level would require large reductions of global CO_2 emissions from current levels. The lower the chosen level for stabilisation, the sooner the decline in global CO_2 emissions would need to begin, or the deeper the emission reduction would need to be on the longer term (IEA, 2011).

Table 1.1 shows the world CO_2 emissions from fossil fuel combustion in 2006 and 2008, with IEA projection for 2020. From Table 1.1, IEA had predicted that the amount of CO_2 emissions will increase by year.

Table 1.1: World CO_2 emissions from fossil fuel combustion in 2006 and 2008, with IEA projection for 2020

Emissions	Growth Rate, 2006-2015	Growth Rate, 2015-2020	CO_2 Emissions, 2006	CO_2 Emissions, 2008	CO_2 Emissions, 2020
By Fuel:	Percent		Million Tons Carbon		
Coal	3.1	1.6	3,185	3,431	4,555
Oil	1.3	0.9	2,937	2,947	3,454
Gas	2.0	1.5	1,484	1,602	1,918
By Sector:					
Power Generation	2.9	1.6	3,119	3,250	4,365
Coal	3.2	1.7	2,273	2,365	3,300
Oil	-0.4	-1.9	241	236	211
Gas	2.8	2.0	605	650	853
Total Final Consumption	1.7	1.1	4,123	4,323	5,090
Coal	2.7	1.1	855	990	1,150
Oil:	1.5	1.2	2,515	2,527	3,033
(i) of which transport	1.7	1.3	1,708	1,746	2,126
(ii) of which marine bunkers	1.0	1.0	159	158	326
(iii) of which international aviation	2.2	1.8	108	124	145
Gas	1.4	1.2	754	807	907
Other Energy Sector			364	406	472
Total CO_2 Emissions	2.2	1.4	7,606	7,980	9,927

Source: IEA (2010)

A strategic plan had been suggested to prevent the environmental and economic collapse as shown in Table 1.2 (Rattan, 2004). Unfortunately, the remediation of CO_2 can be physically stored or chemically transformed, but these methods only overcome the problem temporarily. Thus, CO_2 must be transform into another useful or non-toxic compound in order to solve these problems permanently (Hsiang et al., 2002).

Table 1.2: CO_2 Emissions Reductions and Sequestration in 2020 (Rattan, 2004).

Action	**Amount**
Energy Restructuring	Million Tons of Carbon
Replacing fossil fuels with renewables for electricity and heat	3,210
Restructuring the transport system	1,400
Reducing coal and oil use in industry	100
Biological Carbon Sequestration	
Ending net deforestation	1,500
Planting trees to sequester carbon	860
Managing soils to sequester carbon	600
Total Carbon Dioxide Reductions in 2020	**7,670**
Carbon Dioxide Emissions in 2006	9,350
Percent Reduction from 2006 Baseline	**82.0**

Source: Rattan (2004)

Fujishima and Honda (1972), had discovered the photocatalytic splitting of water on titania (TiO_2) semiconductor electrode. Due to the new discovery of the usage of semiconductor, the researchers pay more attention towards it as a medium in photocatalysis activity for environmental protection (Hsiang et al., 2002). Photocatalysis is a catalytic process that occurs on the surface of semiconductor materials under the irradiation of photons (Fujishima and Honda, 1972). Yamashita et al., (1998) identified that photocatalysis has been exploited for various environmental process such as deodorization, water purification, air purification, sterilization and soil proof. In addition, Yamashita et al., (1998) had proven that CO_2 has been reduced

efficiently with water by photocatalysis. Thus, the photoreduction process is suitable to be use to reduce the concentration of CO_2.

Photoreduction is one of the methods which can be used to reduce the concentration of CO_2 gas and convert it to become non-toxic and reusable hydrocarbon resources. In this process, the solar energy had been use as an energy input because it can be supplied naturally and due to its abundant (Wu and Chih-Yang, 2001). Photoreduction by using TiO_2 photocatalyst is being widely studied as a relatively new technique of pollution abatement. TiO_2 is a commonly used photocatalyst because of its stability in an ultraviolet (UV) light and water (Wan-Jian et al., 2010). However, the need of UV excitation source restricts its technological utility for limited applications. For widespread applications, TiO_2 photocatalyst effective in solar light or light from visible region of the solar spectrum need to be developed as future generation photocatalytic material. TiO_2 absorbs only 5 % energy of the solar spectrum hence numerous studies have been performed to extend the photoresponse and photocatalytic activity by modifying its crystal growth, doping and heterostructuring design of high-efficiency semiconductor photocatalysts which have substantial influences on light-response range, redox potentials of photoinduced charge carriers, and bulk and surface separation probability of the photocatalysts (Gang et al., 2009).

Significantly, the crystal growth is a key parameter in controlling the phase, shape, size, crystallinity and surface area of TiO_2 photocatalysts. Soria et al., (2003) claimed that the surface of TiO_2 photocatalysts have a substantial influence on modifying electronic structure and the construction of heteroatomic surface structures modification by doping with organic polymers, metal and non-metal ions has been proven to be an efficient route to improve the photo-catalytic activity of TiO_2 under solar light irradiation (Gang et al., 2009). Many researchers have paid attention in developing modified TiO_2 powder catalyst but using the powder catalyst has the disadvantages like stirring during the reaction and separation of catalyst after each run (Zhang et al., 2003).

According to Lee et al., (2005), metal oxide has attracted increasing attention due to its effectiveness in realizing visible-light photocatalytic activity of wide bandgap

semiconductor photocatalysts. Besides that, according to Gang et al., (2009), the other key factors in adjusting the spectral distribution of the induced electronic states of those dopants and reconstructing favorable surface structure of the photocatalysis is the chemical states and locations of dopants. Heterogeneous or heterostructures of TiO_2 photocatalysts seem to possess advantages in more efficiently utilizing solar light by combining different electronic structures than a single phase semiconductor photocatalysts (Gang et al., 2009). The interrelationship among the key factors in crystal growth, doping and heterostructuring of TiO_2 semiconductors for photocatalysis is illustrated schematically in Figure 1.1.

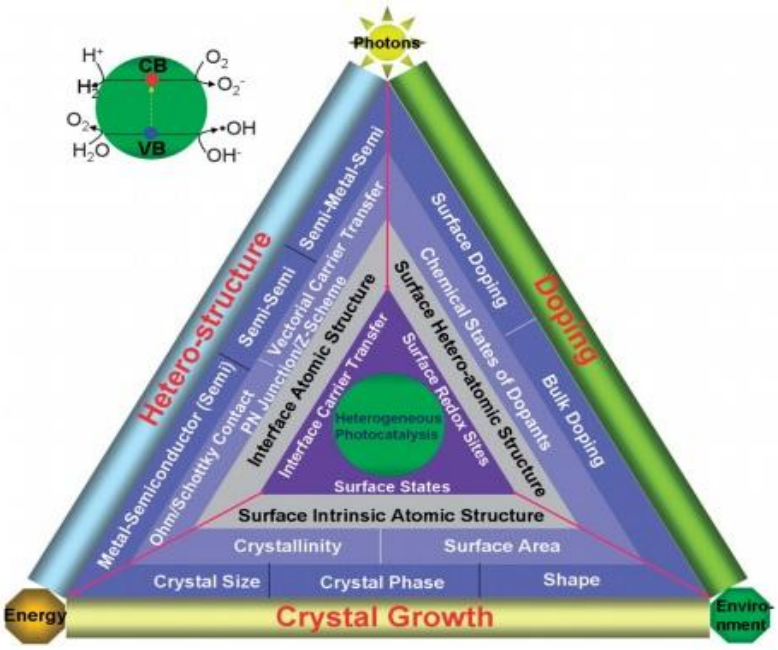

Figure 1.1: Correlation of key factors in crystal growth, doping and heterostructuring of semiconductors for photocatalysis. (CB: conduction band; VB: valence band)

Source: Gang et al., (2009)

Furthermore, the movement electron and hole from one component unit to another with appropriate band edge positions can significantly decrease the electron-hole recombination probability and increase the lifetime of charge carriers, thus enhanced the efficiency of the photocatalytic activity (Paola et al., 2004). Therefore, it will increase the photoactivity of TiO_2. In this research, Aluminium Oxide (Al_2O_3) was

used as the source of metal oxide loaded on TiO_2 by using two methods which are sol gel method and hydrothermal method.

1.2 Problem statements

Carbon dioxide (CO_2) is a major source of the greenhouse gas effect which causes the increasing in the Earth's temperature. The concentration of atmospheric CO_2 has increased by about 35 % since the beginning of the age of industrialization. This is due to the globalization and human activities such as the combustion of fossil fuels and deforestation. In order to solve this matter, the researchers work hard to find the best remediation for this problem. One of the best method uses is to develop a heterogeneous catalyst.

The aim of this study is to prepare and characterize the metal oxide loaded Titania (heterogeneous catalyst) by using two different methods which are the sol gel method and hydrothermal method in order to enhance the properties of Titania so that the photocatalytic activity in photoreduction process can be increase.

1.3 Research Objectives

The main objectives of this study are to:

a) Prepare Al_2O_3-TiO_2 as a catalyst to be used in photoreduction process.
b) Characterize the prepared Al_2O_3-TiO_2 and pure TiO_2 catalyst for it physical and chemical properties.

1.4 Scope of Research

This study will focus in two main areas that are;

i. To prepare a metal oxide loaded on TiO_2 and pure TiO_2 using two different methods which are sol gel method and hydrothermal method.

ii. To characterize the chemical and physical properties of the prepared catalysts by using Scanning Electron Microscope (SEM), Fourier Transform Infrared Spectroscopy (FTIR), X-Ray Diffraction (XRD) and Brunauer-Emmett-Tellar (BET) method.

1.5 Rationale & Significance

In this study, the preparation and characterization of metal oxide loaded Titania in photoreduction process will be investigated. According to Aprile et al., (2008) several factors which affect the efficiencies of a particular metal oxide photocatalyst are including the particle size, crystal phase, purity, band gap, flatband potential, surface treatments, and co-catalysts.

Surface reactions of the heterogeneous catalyst play the important role in promoting the electron-hole pairs separation. The improvement in efficiency of catalytic activity will increase if the surface area of the catalyst is increase. In addition, Paola et al., (2004) also stated that the catalyst should have the electron hole combination and interfacial change transfer. So that the improvement in the separation photoproduced of electron hole pairs can be increased. Thus, it is significant to determine the characteristic of the catalyst so that the efficiency of the photoreduction can be achieve (Slamet et al., 2004).

Navio et al., (1999) suggested that by investigating the characteristic and the best method used in the preparation of the catalyst, the amount of CO_2 produce to our environment can be reduced by photoreduction process.

CHAPTER 2

LITERATURE REVIEW

2.1 Titania (TiO_2)

Hashimoto et al., (2004) reported that the Rossi from USA is the first successful attempt to produce relatively pure titania from ilmenite ore in 1908. TiO_2 is a type of semiconductor which had been widely used as white pigment in the plastic, paint and paper industries. The first titanium pigment company which initially produced composite pigments commenced production is at Niagara Falls in 1918. Another main landmark in the history of TiO_2 is it was develop by using improved method of thermal hydrolysis conducted by Blumenfeld in 1920 in France. The technology was licensed to a number of companies in Europe as well as in USA. The growth of the production and use of TiO_2 white pigments began in the early 1930s and continues until recently. Other than that, it is also used as a UV absorber in sunscreen. Hashimoto, et al., (2004) also claimed that TiO_2 is non-toxic semiconductor so it safe to humans and environmental.

Gao, (2002) investigated that TiO_2 has the most efficient photoactivity, the highest stability and the lowest cost which lead to the increasing use of TiO_2 as a photocatalyst for pollution reduction due to its strong oxidizing power, stable at different pH and favorable band gap energy. Paola et al., (2004), asserted that TiO_2 plays the important roles in promoting the reduction of CO_2. It is use to support the materials for metal or metal oxides due to its ability to modify the catalytic properties of the supported phase (Slamet et al., 2004).

Lusvardi et al., (1998) claimed that titanium cations are present in a variety of different coordination environment and oxidation states. The numerous surface valence states of TiO_2 are capable of interacting with adsorbed species in unique ways facilitating many different chemical reactions. Sherill et al., (2001) mentioned that surface oxygen plays an important role in the state of titanium surface atoms. Fully oxidized surfaces show traits similar to the transition metal complexes. Moreover, the fully oxidized surface has insulator properties with very low electrical conductivity. The removal of surface oxygen causes electron transfer into the 3d orbital. Therefore at non-zero temperatures, electrons can be thermally excited to conduction band creating a more conductive surface. Surface oxygen can be removed creating vacancies via several methods which are, annealing in hydrogen, annealing in vacuum (Lusvardi et al., 1998) and argon sputtering under ultrahigh vacuum conditions (Sherrill et al., 2000). This creates a useful material for catalytic and gas sensing applications (Erkan et al., 2006).

2.1.1 Crystalline structure of TiO_2

TiO_2 particles are referred as primary, aggregates or agglomerates. Primary particles are the single crystals that are bound by crystal planes. Meanwhile, aggregates are the sintered primary particles that are connected by a crystals faces. Agglomerates are multiple primary particles and aggregates that are held together by van der Waal's forces. The diameter of the particles which had been scattering by TiO_2 with the presence of light is maximized with 0.2-0.3 μm and most commercial products that are used as pigments have primary particles size within this range. Besides that, the range of ultrasonically dispersed primary particles and aggregates is narrow and generally ranges from < 0.1 to 0.5 μm (Swiler, 2005).

Supan et al., (2011) stated that TiO_2 has three kinds of different crystal structure forms which are anatase, brookite and rutile. They are all composed of octahedral groups of oxygen atoms around titanium (Ti) exhibiting the characteristic six coordination of this element. However the position in which the groups are linked together is different for each mineral (Bragg et al., 1965).

Crystalline structure of rutile as shown in Figure 2.1 has a dimension of 4.58 Å, while the c dimension is 2.95 Å with 6:3 coordination. From Figure 2.1, every Ti atom is surrounded by oxygen atoms approximately at the corners of a regular octahedron and every oxygen atom by three Ti atoms approximately at the corners of an equilateral triangle. This atomic arrangement is one of the standard types for AB_2 compounds in which the atom is in six-coordination and it is also characteristic of a very large number of crystals. The crystal form structure of rutile can be seen at Figure 2.2.

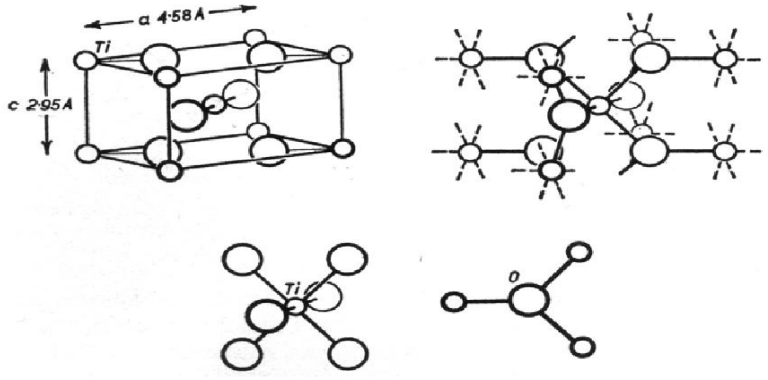

Figure 2.1: The structure of rutile. Above (left) unit cell and (right) bonds between Ti and O atom. Below environment of Ti and O atoms

Source: Alp (2009)

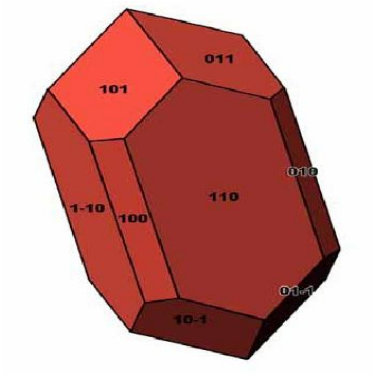

Figure 2.2: Crystal form structure of rutile

Source: Alp (2009)

For anatase, it has 3.78 Å as its dimension and 9.50 Å as it c dimension as shown in Figure 2.3. From Figure 2.3(a), it shows the position of the atoms in the body-centered unit cell. While Figure 2.3(b), shows the links between Ti and O atoms. As in rutile, shows in Figure 2.3(c), every Ti atom is between six O atoms and every O atom is between three Ti atoms. Anatase and rutile are thus alternative forms of 6:3 coordination. The crystal form structure of anatase can be seen at Figure 2.4.

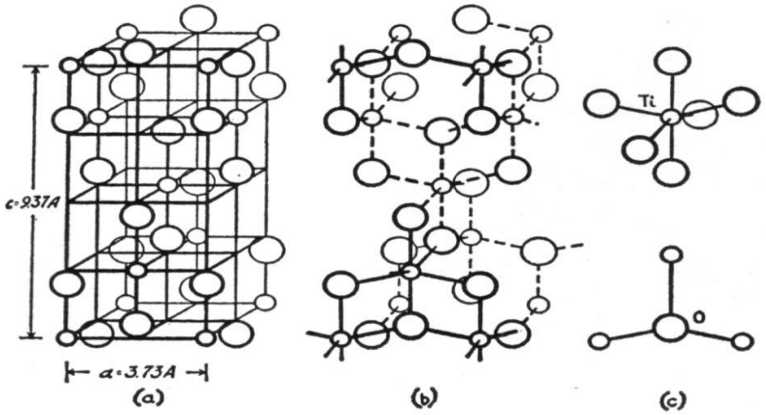

Figure 2.3: The Structure of anatase (a) Unit cell (b) bonds between Ti and O, (c) environments of Ti and O atoms which are closely similar to those in rutile

Source: Alp (2009)

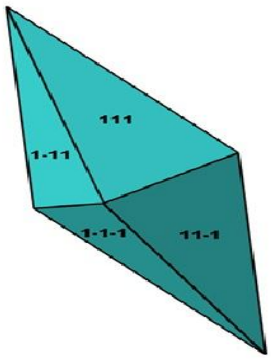

Figure 2.4: Crystal form structure of anatase

Source: Alp (2009)

Meanwhile, for brookite, it has an orthorhombic structure and its a, b, and c dimensions are 9.14 Å, 5.44 Å and 5.15 Å. The structure is shown in an idealized form in Figure 2.5 and it can be seen that the structure is quite complex compared to the other polymorphs.

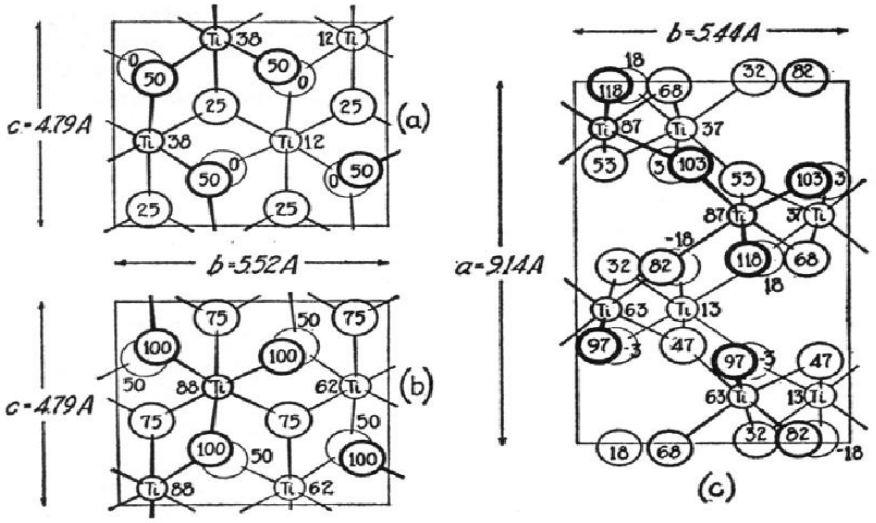

Figure 2.5: The structure of brookite in idealized form. (a) The oxygen atoms at height 50 being common to both (b) is to be superimposed on. (c) The actual structure projected on (001). Oxygen atoms which should be superimposed have been displaced symmetrically

Source: Alp (2009)

As in rutile and anatase, each Ti atom is surrounded by an octahedral group of oxygen atoms. In all three forms of TiO_2, the titanium-oxygen distance lies between 1.9 Å and 2 Å. Neighbouring oxygen atoms are between 2.5 Å and 3 Å apart, the smaller distance obtaining when the pair of oxygen atoms is linked to the same two titanium atoms. The crystal form structure of anatase can be seen at Figure 2.6.

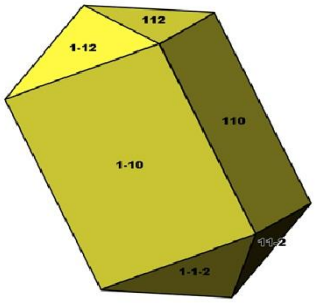

Figure 2.6: Crystal form structure of brookite

Source: Alp (2009)

Chen et al., (2003), claimed that anatase and brookite are meta-stable phases and irreversibly transform to the thermally stable rutile phase upon heat treatment in the temperature range from 450 °C to 900 °C. Better crystallinity and larger crystallite size of catalyst also can be obtained at the same time. Many studies have clarified that anatase exhibited greater photocatalytic property than rutile due to the highly hydroxylate surface responsible for photocatalytic reaction which is readily formed in the anatase structure. Anatase nanoparticles can be fabricated into various device forms for solar cell and fuel cell applications. Therefore, the stabilization of anatase phase becomes a subject of interest to be studied (Qui, 2006).

2.1.2 Capacity, Production and consumption of TiO_2

Linak and Inoguchi (2005) revealed that in 2004, the world production of titanium mineral concentrates had increased to 5.2 million tonnes from 4.6 million tonnes in 2000. Approximately 95 % is used as feedstock for TiO_2 and the remainder is used in titanium metal alloys. In 2004, South Africa (25 %) is the main leading supplier of titanium feedstock followed by Australia (21 %), Canada (14 %), China (8 %), The Ukraine (7%) and Norway (7 %). Approximately 60 plants sites worldwide produce TiO_2 with an average annual capacity of 60000 tonnes. Table 2.1 represents the world TiO_2 capacity by region and process (Linak and Inoguchi, 2005).

Table 2.1: World capacity of TiO_2 (thousand tonnes, gross weight)

Region	1993			1998			2002			2005		
	S	C	Total	S	C	Total	S	C	Total	S	C	Total
North America	202	1288	1488	178	1436	1614	134	1656	1790	80	1717	1797
Central and South America	55	0	55	60	0	60	60	0	60	96	0	96
Western Europe	875	317	1192	913	405	1318	925	472	1397	862	547	1409
Central and eastern Europe	195	0	195	203	0	203	217	0	217	234	0	234
Africa and Middle East	35	50	85	40	80	119	40	100	140	25	100	125
Japan	270	50	319	272	52	324	259	68	327	240	68	308
China	–	–	–	–	–	–	258	408	666	658	15	673
Oceania and other Asia	224	114	338	291	184	475	–	–	–	141	404	545
Total	1856	1819	3672	1957	2157	4113	1893	2704	4597	2336	2857	5187

Where, C: Chloride process

S: Sulfate process

Source: Linak and Inogouchi (2005).

TiO_2 is used in more than 170 countries. The major exporting regions are North America and Australia and most of the countries in the rest of the world are net importers. Table 2.2 shows the world supply and demand for TiO_2 until 2004 (Linak and Inoguchi, 2005).

Table 2.2: World Production and consumption of TiO_2 (thousand tonnes, gross weight)

Region	1997		2001		2004	
	P	C	P	C	P	C
North America						
Canada	75	105	68	90	76	104
Mexico	102	37	124	65	124	64
USA	1340	1129	1340	1100	1511	1162
Central and South America						
Brazil	79	108	78	111	80	124
Other	0	60	0	60	0	85
Western Europe	1113	1099	1150	1100	1254	1183
Central and eastern Europe	136	125	155	155	155	155
Africa and Middle East						
Saudi Arabia	50	10	55	10	90	30
Other Middle East	0	60	0	65	0	120
South Africa	30	25	30	20	20	28
Other Africa	0	15	0	35	0	45
Japan	241	269	257	246	253	238
Oceania and other Asia						
Australia	160	40	181	66	200	40
China	102	170	147	256	350	540
India and Pakistan	50	70	44	77	52	82
Indonesia	–	–	–	–	0	49
Malaysia	–	–	50	28	50	15
Philippines	–	–	–	–	0	33
Republic of Korea	35	100	42	118	40	120
Singapore	–	–	41	16	45	30
Southeast Asia	77	145	–	–	–	–
Taiwan (China)	68	71	123	66	120	66
Thailand	–	–	–	–	0	71
Other	–	–	0	108	0	29
Total	3658	3638	3885	3792	4420	4423

Where, C: Consumption

P: Production

Source: Linak and Inogouchi (2005)

2.1.3 Photoinduced Properties of TiO_2

TiO_2 is an important photocatalytic semiconductor which has some unique properties and its photocatalytic increases remarkable at nanoscale. TiO_2 will produce a pairs of electrons and holes when it absorbs ultraviolet radiation from the sunlight or illuminated source. Marius and Gabriel (2007) claimed that when this situation occurs, the electron valence band of TiO_2 become excited and will promoted the electron to the conduction band of TiO_2. Thus, it will create the negative-electron (e^-) and positive-hole (h^+) pair which called a semiconductor's photo excitation state and at the same time will produce a band gap as shown in Figure 2.7. Therefore, electron-hole pair separation is an important parameter in determining the photocatalytic activity (Cao et al., 1999). Band gap is defined as the energy difference between the valence band and the conduction band. The wavelength of the light necessary for photo-excitation is 1240 (Planck's constant, h)/ 3.2 eV (band gap energy) = 385 nm (Xu et al., 2005).

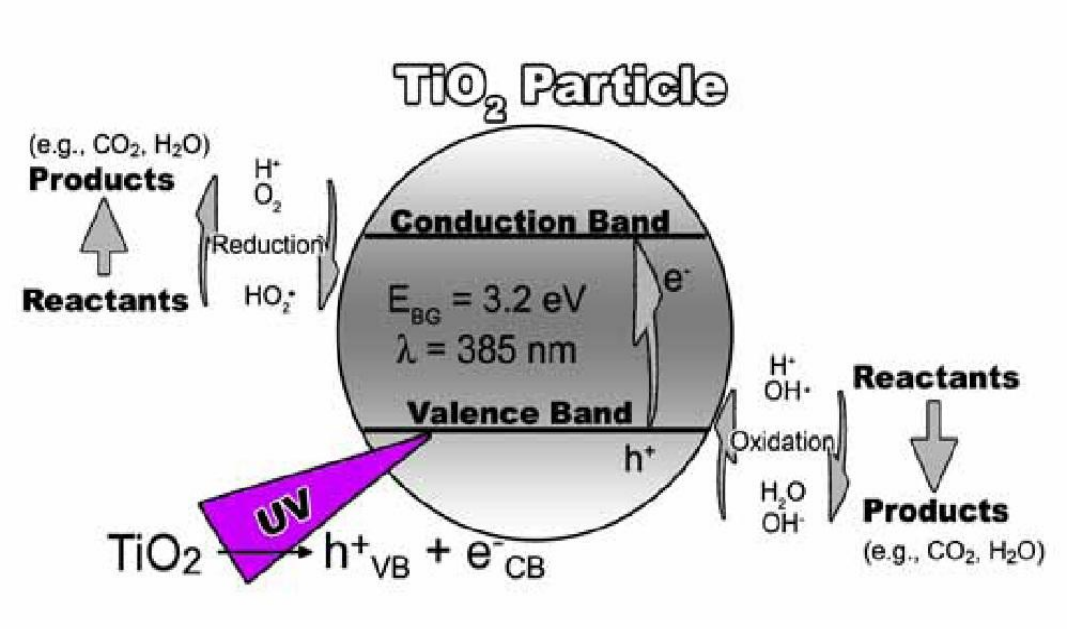

Figure 2.7: Operation of a photochemical excited TiO_2 particle

Source: Marius and Gabriel (2007)

2.1.4 Mechanism of TiO_2

The general equation of a photocatalyzed reaction can be given as shown in equation 2.1.4.1. Where $(Ox)_{ads}$ is the adsorbed oxidant and $(Red)_{ads}$ is the adsorbed reducer.

$$Ox_1)_{ads} + (Red_2)_{ads} \rightarrow Red_1 + Ox_2 \qquad (2.1.4.1)$$

The reaction can be either oxidation or reduction reaction which depends on the sign of Gibbs free energy. According to Hoffman et al., (2005), general mechanism that had been proposed for heterogeneous photocatalysis on TiO_2 is listed below:

(a) Adsorption of Organic Materials:

Organic $\rightleftarrows RX_{ads}$ Where, RX_{ads} represents the organic substrates.

(b) Electron transfer from either the adsorbed substrate (RX_{ads}) or the adsorbed hydroxyl radicals ($^{\cdot}OH_{ads}$) to the holes h^+:

$h^+ + RX_{ads} \rightarrow RX^+_{ads}$

$h^+ + H_2O_{ads} \rightarrow {}^{\cdot}OH_{ads} + H^+$

$h^+ + OH^-_{ads} \rightarrow {}^{\cdot}OH_{ads}$

The second and the third one are the most important steps for the major oxidant, adsorbed hydroxyl radicals ($^{\cdot}OH_{ads}$) which generated in these steps.

(c) Molecular oxygen is presented in oxidative decomposition processes due to its electron acceptor in the electron transfer reaction:

$O_2(g) \rightleftarrows O_{2ads}$

$O_{2ads} \rightarrow 2O_{ads}$

$O_{ads} + e^- \rightarrow O^-_{ads}$

$e^- + O_2 \rightarrow O_2^-$

(d) The superoxide anion can further be involved the following reaction and give more ($^{\cdot}OH_{ads}$) group:

$$H^+ + O_2^- + HO_2 \rightarrow H_2O_2 + O_2$$
$$H_2O_2 + hv \rightarrow 2\,^{\cdot}OH$$

(e) The active free radicals ($^{\cdot}OH_{ads}$) oxidize organic substrate (RX_{ads}) adsorb onto the surface of the semiconductor particles.

$$^{\cdot}OH_{ads} + RX_{ads} \rightarrow \text{Intermediate} \rightarrow \text{Alcohols, Ketones, Acids, } CO_2, H_2O$$

The knowledge of photocatalysis mechanism on TiO_2 surface is not complete yet although some models were proposed. In most of the process, the initial steps involving the reactive oxygen species and organic molecules are particular interest where the oxygen acts as primary electron acceptor and the rate determining process is the electron transfer process. Mao et al., (1991) investigated that hydroxyl radical is the principal reactive oxidant in the photocatalytic reactions of TiO_2. H_2O_2 also can act as an electron acceptor or as a direct source of hydroxyl radicals. Hydroxyl radicals, superoxide, hydrogen peroxide and oxygen can play important roles in photocatalyic reactions which depends on the condition of the reaction involve (Stanford et al., 1993)

Fujishima et al., (2000) stated that photocatalysis is a condition where the excited electrons and holes can be used directly to drive a chemical reaction. The less adjacent coordinate atoms and unsaturated sites of the surface atoms of TiO_2 nanoparticles make it more active than the bulk atoms. Moreover, the surface defects can act as a hole trapping centers in the photocatalysis process. With the decreasing in size, the surface to volume ratio is increases and the surface effect become more active and TiO_2 nanoparticles with a high surface volume ratio can be obtained (Murray et al., 2000).

Wang R et al., (1998) claimed that superhydrophilicity is a newly studied photoinduced property of TiO_2 films. The vacancy of the generated oxygen on the photoexcited TiO_2 surface explained the uniformly spreads of water condition on the

UV light illuminated TiO_2 surface. The van der Waals forces hydrogen bonding interactions between H_2O and ^{-}OH are increase due to the following adsorption of water after generation of oxygen vacancies (Nakajima et al., 2001). The Self-cleaning and anti-fogging of TiO_2 surface can be synthesized according to the superhydrophilic effect. Nakajima et al., (1999) claimed that the superhydrophilic of TiO_2 extraordinary property shows promising applications to the preparation of anti-strain architectural materials, anti-fogging glass and accelerated drying material.

Figure 2.8 shows the schematic representation of superhydrophilicity of TiO_2. In Figure 2.8(a), the electrons in the conduction band have the affinity to reduce TiO_2 to form an intermediate species. In the following steps in Figure 2.8(b), the holes in the valence band push away the oxygen atoms and create vacant sites which can be easily created if there are some surface defects. Lastly, in Figure 2.8(c), The TiO_2 with the vacant sites can dissociate water into H and OH groups which leads to superhydrophilicity.

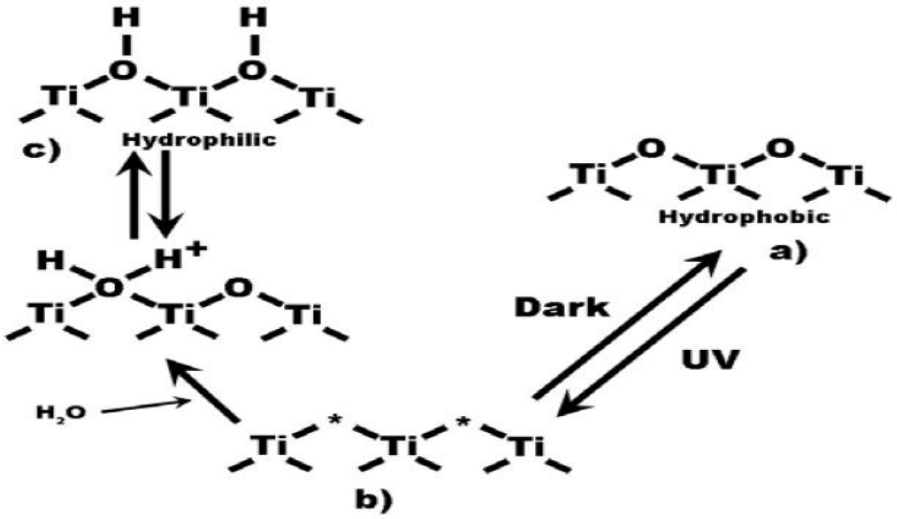

Figure 2.8: Superhydrophilicity of TiO_2 (a) Hydrophobic TiO_2 (b) TiO_2 with vacant sites (c) hydrophilic TiO_2

Source: Alp (2009)

Nishimura et al., (2010) revealed that numerous organic materials can be mineralized into carbon dioxide and water under UV radiation on TiO_2 nanoparticles suspension. The preparation of particles suspension with a high degree of homogeneousness and stability in the aqueous phase is the main key parameter which affecting the photocatalytic reactions. The way to improve the feasibility of organic substance removal is by increasing the stability suspension and the adsorption of various organic molecules onto TiO_2 nanoparticles surface sites (Xu et al., 2003).

Miyauchi et al., (2004) stated that in aqueous systems, nanoparticles of TiO_2 always carry charge due to the ionization, the adsorption ions or the preferential substitution of ions from the particles surfaces. The physical properties of TiO_2 nanoparticles suspensions are mainly dependent on the behaviour of aqueous suspensions. It is especially reactive to the electrical and ionic structure if the particle is in a liquid surface. Zeta potential is used to identify the intensity of repulsive forces among particles and the stability of dispersion. According to Molino et al., (1999), this parameter is the key on the stability control of TiO_2 nanoparticles in suspension and the adsorption properties of TiO_2 nanoparticles sites.

Besides that, Mandzy et al., (2005) stated that some studies showed the isoelectric points (IEP) could be correlated with the photocatalytic activity of TiO_2 particles and the surface charge of TiO_2 particles affected the inactivation kinetics of bacteria considerably. Samples with different chemical compositions had all different zeta potential dependence on pH values of particles (Gumy et al., 2006). Figure 2.9 shows the application of TiO_2 as photocataysts in photoreduction process where it helps to convert CO_2 into a reusable hydrocarbon

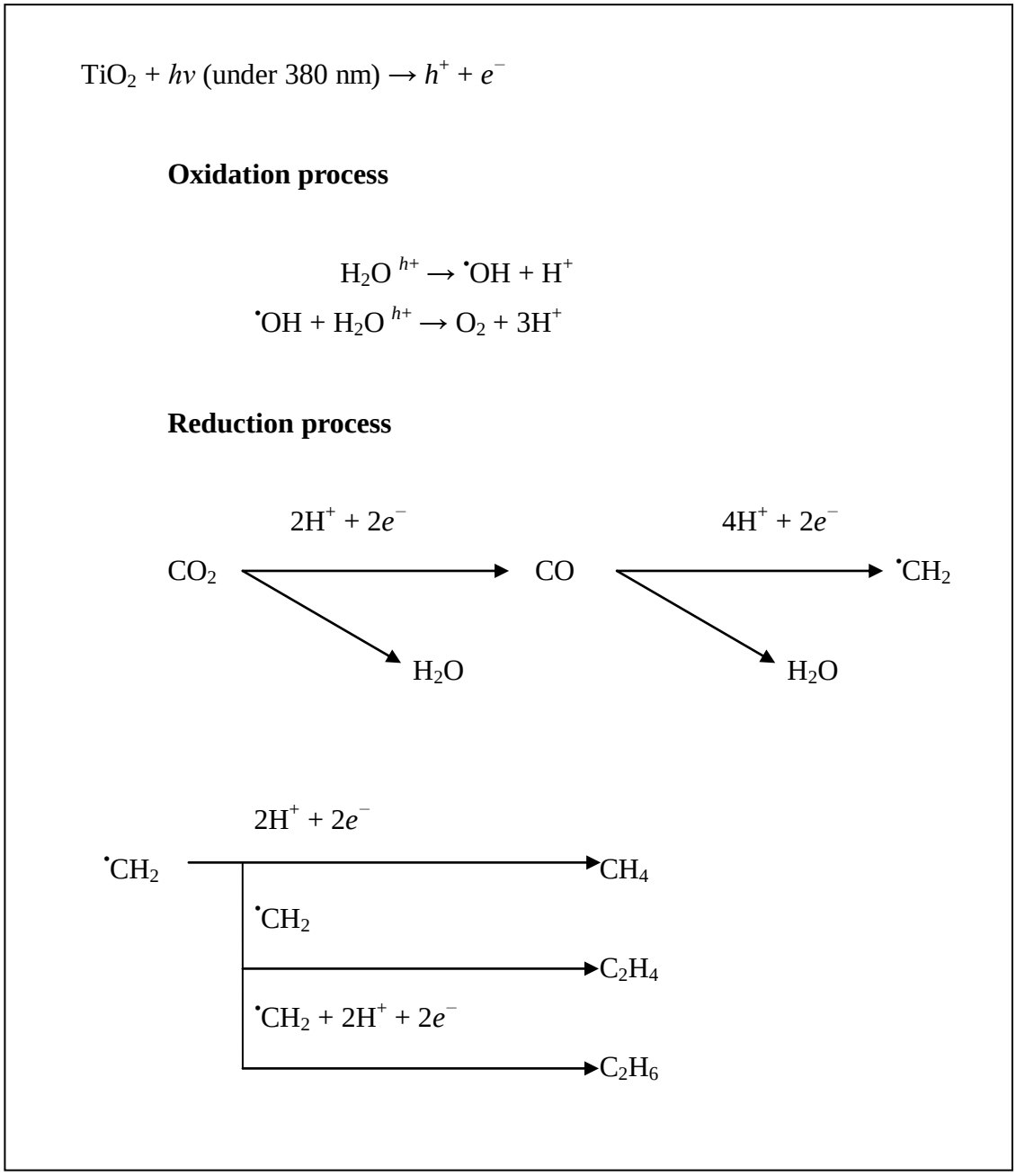

Figure 2.9: Mechanism of photoreduction process

Source: Nishimura et al., (2010)

2.2 Aluminium Oxide (Al_2O_3)

Oberlander (1984) was defined alumina (Al_2O_3) as a white powder that normally produced from bauxite ores. It is one of the most widely used advanced ceramic materials with applications ranges from spark plugs to catalyst materials. Al_2O_3 attractive for engineering applications due to its chemical and thermal stability, relatively good strength and electrical insulation characteristic combined with availability in abundance have made. Other than that, it is also a relatively low cost material, and by using a number of fabrication methods, it can easily be formed and finished. Al_2O_3 has several allotropic forms, but only the usual type or α-alumina is considered. It has an internal crystal structure where the oxygen ions are packed in a closed packed hexagonal (cph) arrangement with aluminium ions in two-thirds of the octahedral sites.

According to Oberlander (1984), there are 27 aluminum chemicals listed as Al_2O_3 which show a wide range of physical and chemical properties of Al_2O_3 in a research conducted by McZura et al. (1978). There are varieties of physical properties of synthetic commercial aluminas which are suitable to be use as adsorbents and catalysts. Aluminas that have a specific area from 0.01 m^2/g to 400 m^2/g, volume of the pores from 0.1 cm^3/g to 1.4 cm^3/g and average pore size from 2nm or 20Å to 177μm are known as “active aluminas” (Pedro et., al 2000).

Oberlander (1984) also revealed that “active alumina” is commonly used in catalyst technology typically means for aluminas that have high surface areas and considerable chemical activities. It also used as a term patented by ALCOA (ALCOA 1969, Goodboy and Downing 1990) which referred to aluminas that exhibit an ability in adsorbing significant quantities of water from gases and liquids. Other than that active aluminas also used in advanced ceramics which is used as a contraction of the term “reactive alumina” (ALCOA, 1972). The reactive aluminas are referring to aluminas which, after pressed without the addition of sintering catalysts and fired at high temperatures which smaller than melting point of Al_2O_3, they will sinter into very hard low-porosity pieces having α-alumina structure.

Hart and Lense (1990) claimed that Al_2O_3, have a large use in the chemical process industry (Hart and Lense 1990), as a catalyst, a catalyst support (Oberlander, 1984) or as an adsorbent (active aluminas) (ALCOA 1969, 1972), due to variety of surface properties or in the advanced and traditional ceramic industries (McZura et al. 1976, Xavier 1997). This is also because of the α-alumina structure itself which considered the remarkable thermal, mechanical and chemical properties of α-alumina. Meanwhile, Tshang et al., (1979) also stated that Al_2O_3 have a high quality optical and di-electric properties and therefore suitable for antireflection coatings on a semiconductors. Table 2.3 and Table 2.4 show the general properties of Al_2O_3.

Table 2.3: Physical properties of Al_2O_3

Thermal Conductivity (W/m-K)	28 - 35
Thermal Expansivity, (m/m-K)	8.0×10^{-6}
Upper Continuous Use Temperature (°C)	1800

Source: Panayiotis and Marc-Jean (1995)

Table 2.4 Chemical properties of Al_2O_3

Melting Point (°C)	2000 ± 30
Density at Room Temperature (g/cm^3)	3.9
Apparent Porosity (%)	0
Water Absorption-Saturation (%)	0

Source: Panayiotis and Marc-Jean (1995)

2.3 Synthesis of TiO_2 nanoparticles

Navio et al., (1999) stated that, the preparation method use to prepare the catalyst is one of the most important factors that affecting the efficiency of the photoreduction activity. So, the methods use to prepare the catalyst are very important things that need to be considered. Akurati et al., (2006), identified that the photocatalytic activity of TiO_2 are strongly dependent on its crystal phase, particle size, cystallinity, surface area, pore size and distribution. Surface area and porosity are very

important parameters that need to be considered for TiO_2 photocatalysts to acts as good catalysts with a high surface area and porosity which brings a better photoactivity (Alp, 2009). However, TiO_2 with classic synthesis methods does not have that much of surface area. Thus, by converting TiO_2 particles to nanoparticles with different shapes and also synthesizing them with a template will help to enhance the porosity and the surface area of the photocatalyst (Gang et al., 2009).

Saponjic et al., (2005), reported that there are many studies conducted by a lot of researchers with the objective in aiming the control of size and shape of inorganic nanoparticles. Most common methods used are sol-gel, hydrothermal, chemical vapour deposition techniques and etc. In a research conducted by Chemseddine and Moritz (1999) they are able to the elongated of TiO_2 nanocrystals which were synthesized from the hydrolysis reaction of titanium alkoxide. Meanwhile, according to Joo et al., (2005), short and long nanorods, bullet and diamond shaped nanocrystals, platelets, nanotubes and fractals have been prepared. Manna et al., (2002) claimed that the modulation of surface energies of different crystal facets with the use of surfactants explained the shape evolution on anatase TiO_2 nanocrytals from bullet and diamond shape to rod structures.

Li et al., (2005) stated that TiO_2 nanotubes have attracted a wide attention for their potential applications in high efficiency photocatalysis and photovoltaic cells. Sol gel method is used in various studies to synthesize the well aligned of TiO_2 nanotubes. Wang et al., (2002) developed a one step templating synthesis of TiO_2 arrays in solutions which proposed a model for the formation of TiO_2 nanotubes. In this model, TiO_2 nanotubes were formed following a three dimensional lamellar TiO_2 is keys for the formation of TiO_2 nanotubes. Li et al (2005), claimed that by controlling the immersion time of template membrane in precursor sol TiO_2 nanotubes or nanofibers could be obtained. Other than that, by using a soft chemical process TiO_2 nanotubes from layered titanate particles also could be obtained (Wei et al., 2005).

Burda et al., (2005) investigated that by synthesized at low temperature, it had successfully prevent the agglomeration and excessive growth of TiO_2 particles,

crystallized anatase and rutile TiO_2 nanoparticles. Other than that, to obtain a mesoporous TiO_2 some carbon templates can also be used to synthesize the TiO_2 particles. Alexakia et al., (2009) reported that during the synthesis of the templates for instance, activated carbon (Li et al., 2006), poly (alkylene oxide) block copolymer (Fua et al., 2009), polystyrene or hexadecylamine can be added to the medium. In the process, TiO_2 network will cover those templates and after calcinations those templates were gasify and thus leaving pores behind which made the material becomes more porous (Alexakia et al., 2009)

Dongliang et al., (2009) also reported that carbon can be used a doping material to sensitizes TiO_2 and reduces the band gap TiO_2 thus increasing the photocatalytic activity of TiO_2 under visible light irradiation. Based on the literature, some carbon sources were used as doping materials are resins (Dongliang et al., 2009), ethylene glycol (Kar et al., 2009) and carbon nanotubes (Gao et al., 2009). Table 2.5 and Table 2.6 shows the types of dopants used and the preparation methods to produce the doped-titania photocatalysts.

In the other hand, to increase the photocatalytic effectiveness of TiO_2, it can be synthesized with SiO_2. Very effective catalysts can be made by dispersing TiO_2 nanoparticles on high surface area materials like SiO_2 aerogels. Zhu et al, (2009) claimed that SiO_2 aerogel/TiO_2 composite has a much higher photocatalytic activity for increased hydrophilicity. The presence of silica mixed TiO_2 in a well defined amount enhances both the photocatalytic activity and superhydrophilicity due to an increase of the acidity of the surface which means that SiO_2/TiO_2 matrix acts as an adsorber (Guan, 2005) and the situation had been confirmed by further research conducted by Zhang et al (2009) and Bennania et al (2009). With a conclusion if adsorption of organics is increased the photocatalytic activity also will increase.

Kumar et al., (1992) stated that among them, sol gel method which is based on the hydrolysis and polycondensation of various titanium molecular precursors in aqueous solutions or an organic solvent have been shown to be especially versatile synthesis procedures as it produced the catalyst with extremely high surface area. Meanwhile, hydrothermal method shows a great promise in producing a nano particles

size since the products prepared by this method have well crystalline phase which beneficial to thermal stability of the nanosized material (Zhu et al., 2004). Therefore, in this research the Al_2O_3-TiO_2 and pure TiO_2 powder catalysts were prepared by using both sol gel method and hydrothermal method.

Table 2.5: Types of metal dopants materials and preparation methods of doped-Titania Photocatalysts

Kind of dopant	Doped element	Preparation method	Potential application	References
Metal Dopants	Ag	Silver nitrate was mixed with reduction agent (sodium citrate tribasic dihydrate) and the reaction temperature was raised to 80 °C with continous stirring. Then TIP and HNO_3 were added and the reaction was maintained at 50 °C for 24 h. The prepared sol was dried at 105 °C for 24 h and calcined at 300 °C.	Degradation of nitrophenol in aqueous phase	Lee et al., (2005)
	Fe	The reactive magnetron sputtering method: 99 % titanium target and 99.9 % iron pieces were placed in the reaction chamber and mixture of argon and oxygen was introduced into the chamber during discharging.	Wastewater decoloring	Carneiro et al., (2005)
	V	Sol gel method: Solution 1 (vanadyl acetlyacetonate dissolved in n-butanol) was mixed with solution 2 (acetic acid in titanium butoxide) and hydrolyzed (24 h) by the water generated via the estrification of acetic and butanol. The suspension as dried at 150 °C pulverized and calcined at 400 °C for 0.5 h.	Wastewater decoloring	Wu et al., (2004)
	Au	Titanium (IV) butoxide dissolved in absolute ethanol was added to solution containing tetrachloroauric acid ($HAuCl_4.4H_2O$), acetic acid and ethanol. The resulting suspension was aged (2 days), dried under vacuum, grinding and calcined at 650 °C.	Wastewater decoloring	Li et al., (2001)
	Pt	Photoreduction process: TiO_2 was suspended in a mixture of hexachloroplatinic acid in methanol. The suspension was irradiated with a 125 W mercury lamp (60 min). Pt-TiO_2 was separated by filtration, washed with distilled water and dried at 100 °C for 24 h.	Wastewater decoloring	Li et al., (2002)

Table 2.6: Types of non-metal dopants materials and preparation methods of doped-Titania Photocatalysts

Kind of dopant	Doped element	Preparation method	Potential application	References
Non-metal Dopants	N	Titanium nitride (TiN) oxidation: Heating of TiN at 450 - 550 ℃ for 2 h in air (heating and cooling temperature rate: 2 ℃/min).	Photooxidation of aromatic compounds	Wu et al., (2008)
		Treating anatase TiO_2 powder ST01 in NH_3 (67 %)/ Ar atmosphere at 600 ℃ for 3h.	Photooxidation of acetaldehyde in gas phase.	Asahi et al., (2001)
	S	Oxidation annealing of titanium disulfide (TiS_2) at 300-600 ℃	Wastewater decoloring	Takeshi et al., (2006)
	N and S	Hydrolysis of $Ti(SO_4)_2$ in NH_3 aqueous solution, Precipitate was centrifuged , washed with distilled water and alcohol. Obtained gels were dried under vacuum at 80 ℃ for 10 h and were ground to obtain xerogel. The xereogel was calcined at 400-800 ℃ in air for 3 h.	Photooxidation of volatile compounds in gas phase	Yu et al., (2005)
	C	Sol gel method: TBOT was hydrolyzed in the presence of ethanol, water and nitric acid. Precipitated titanium hydroxide was dried at 110 ℃ and calcined in air at 150-200 ℃.	Degradation of Nox: Wastewater decoloring	Treschev et al., (2008)
		Acid catalyzed sol gel process. Alkoxidide precursor was dissolved in corresponding alcohol, mixed with hydrochloric acid aqueous solution. Obtained gel was aged for several days and calcined in air (3 h at 65 ℃ and 3 h at 250 ℃) and grounded.	Photooxidation of phenol compounds in aqueous phase	Lettmann et al., (2001)
	B	Anatase TiO_2 powder was grinding with boric acid triethyl ester and calcinated in air at 450 ℃	Photooxidation of phenol compounds in aqueous phase	Zaleska et al., (2007)
	P	Sol gel method: TIP was hydrolyzed in the presence of isopropanol and water. After hydrolysis phosphoric acid was added. Dispersion was stirred for 2 h, centrifuged at 3500 rpm and dried at 100 ℃. Obtained powder was calcined at 300 ℃.	Photooxidation of phenol compounds in aqueous phase	Korosi et al., (2006)

2.3.1 Sol Gel Method

Nowadays, Sol gel method have become very popular recently due to their high chemical homogeneity, low processing temperatures, and the possibility of controlling the size and morphology of particles (Subramanian et al., 2008). Sol gel provides excellent matrices for a variety of organic and inorganic compounds when the material is derived. One of the most important features of this method is its ability to preserve the chemical and physical properties of the dopants. Thus, make it as a unique host for a biologically important molecule which can be apply in biomedical aspects. A general process scheme of sol gel synthesis is shown in Figure 2.10.

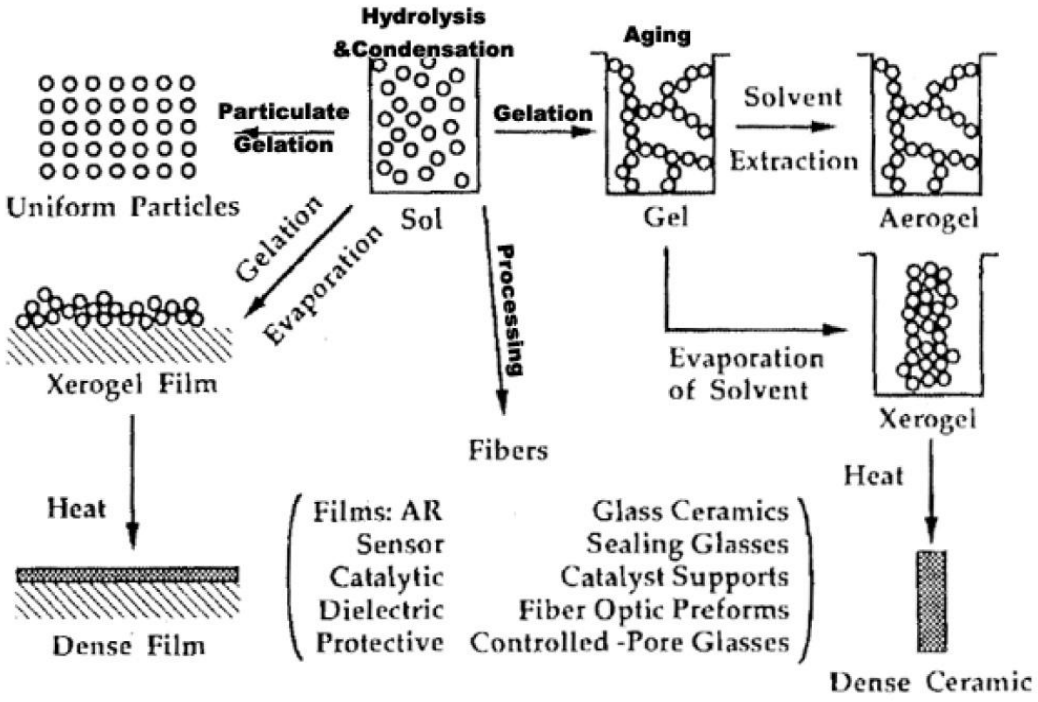

Figure 2.10: Process scheme of sol gel synthesis

Source: Alp (2009)

Sol gel method has been widely used in the synthesis of TiO_2 nanoparticles. In the synthesis of TiO_2 nanoparticles with sol gel method, titanium alkoxide or non-alkoxide can be used as titanium precursors. Titatinum-tetra-isopropoxide ($Ti(OC_3H_7)_4$) (Tonejc et al., 2001), titanium tetrachloride ($TiCl_4$) (Sivakumar et al., 2004) and titanium butoxide $Ti(OBu)_4$ (Yang et al., 2002) are the most commonly used alkoxide

precursors. In this processes, TiO_2 is usually prepared by the reactions of hydrolysis and polycondensation of titanium alkoxide, (TiOR)*n* to form oxopolymers, which are transformed into an oxide network. These reactions can be schematically represented as shown in equations (2.3.1.1), (2.3.1.2), (2.3.1.3) and (2.3.1.4). The reaction started at equation (2.3.1.1). The reactions are proceed until titanium ($Ti(OH)_n$) is formed as shown in equation (2.3.1.2). Then the polymerization reactions take place and produce condensation dehydration. The dealcoholation at equation (2.3.1.3) are occurred after undergo the condesnsation dehydration. The overall reactions of sol gel mechanism are shown in equation (2.3.1.4).

$$Ti(OR)_n + xH_2O \rightarrow Ti(OH)_x(OR)_{n-x} + xROH \quad (2.3.1.1)$$

$$Ti(OR)_n + Ti(OR)_{n-1}(OH) \rightarrow Ti_2O(OR)_{2n-2} + H_2O \quad (2.3.1.2)$$

$$2Ti(OR)_{n-1}(OH) \rightarrow Ti_2O(OR)_{2n-2} + H_2O \quad (2.3.1.3)$$

$$Ti(OR)n + n/2\ H_2O \rightarrow TiO_{n/2} + nROH \quad (2.3.1.4)$$

Wu et al., (2002) stated that condensation reactions will pull the particles together into a compact form and build up the metal oxide crystal. The gelation of the solute occurs after the condensation reaction and form a three dimensional network of gel. The structure of the final products is controlled by the gelation process step which made it as a critical step for method. The network starts to lose water and alcohol when the gel is formed which cause the gel to shrink and creates a pores. During the synthesis, there are various factors that can change the morphology of TiO_2 nanoparticles. Li et al., (2003) reported that the type of titanium precursor (Ois and Ginzberg (1998), the pH value and stoichiometry of the reactants (Li et al., 2003) are the factor that affected the structure of the TiO_2 particles as shown in Table 2.7.

In addition, according to Sugimoto et al., (2003) the chemical complexation in the sol gel system, drying processes and calcinations temperature (Uekawa et al., 2002) are also important parameters that need to be considered. The structure of the dried material is amorphous so in order to crystallize the inorganic material it should be calcined. Alap (2009) claimed that the calcinations temperature is a main important key to obtain a specific crystal structure. The control of the temperature is essential because if the temperature is very high, the material may sinter which is not wanted. Calcination

at high temperatures leads to decrease in surface area, loss of hydroxyl groups and growth of crystal size. Recently, Al-Salim et al., (2000) reported that there are some research conducted which showed that TiO_2 can be crystallized at lower temperature.

Table 2.7: Crystalline size and specific surface area of TiO_2 sample prepared via sol gel method annealed at 400 °C

pH	Sample code	Crystallite size (nm)	Specific surface are (m^2/g)
1	C400-1	13.6	112.8
3	C400-3	8.2	187.4
5	C400-5	7.9	193.8
7	C400-7	9.0	171.7
9	C400-9	8.4	184.2

Source: Siti and Srimala (2010)

2.3.2 Hydrothermal Method

Meanwhile, for hydrothermal method, Vijayan et al., (2010) stated that the hydrothermal process is eco-friendly since it is carried out in a closed system and the contents can be recovered and reused after cooling down to room temperature 112. Other than that, it produces low energy consumption as the equipment and processing required are simple and easy. In addition, Zhu et al., (2004) also agreed that various crystalline products with different composition, structure and morphology could be obtained by controlling hydrothermal temperature and duration of the treatment.

Moreover, fine particle size also can be obtained with more uniform distribution and high dispersion either in polar and non-polar solvents. In this way the energy band structure becomes discrete and TiO_2 nanoparticles exhibit improved optical and photocatalytic properties (Vijayan et al., 2010). The operating condition of hydrothermal treatment processes is usually under 250 °C and the pressure in the autoclave reaches to 2.0 to 6.0 atm. Kominami et al., (2003), investigated that a complete hydrolysis could be obtained in the autoclave without adding excessive water. The main parameter in hydrothermal method is shown as in Table 2.8. The read color indicates the best parameter results in hydrothermal method.

Table 2.8: Effects of synthesis parameter in hydrothermal method

Parameters		Phase formed	Particle size (nm)	Wavelength maximum (nm)
Water: Ethanol	25:75	A	10	390
	50:50	A	16	410
	75:25	A	31	391
Hydrothermal Temperature	60	A	23	397
	80	A	13	415
	100	A	26	393
	120	A, R	41	390
Hydrothermal Treatment duration	6 h	A	21	395
	12 h	A	12	401
	18 h	A	17	410
	24 h	A	29	392

Source: Vijayan et al. (2010)

2.3.3 Other Synthesis Methods

TiO_2 can be synthesized with various methods. Since their details are beyond the focus of this study, they will be explained briefly. One of the methods used is the aerosol process. Aerosol process yields a high-purity of TiO_2 products and does not involve multiple steps, but the high temperature employed in the aerosol process leads to aggregation of the particles. Thus, it is not a good method to produce TiO_2 nanoparticles (Nagaveni et al., 2004).

Another method used is the precipitation method. In precipitation methods, hydroxides are precipitated by addition of a basic solution to a raw material followed by calcinations to crystallize the oxide. The drawback of these methods is the difficulty in controlling the particle size and size distribution of the products. Uncontrolled precipitation often causes formation of larger particles instead of nanoparticles (Borse et al., 2002).

Borse et al., 2002 reported that in the case of using the inert gas condensation process to produced TiO_2 nanoparticles, the process were carried out completely under ultrahigh vacuum conditions and the cost of production by using thise method also is high. Meanwhile, Eriksson et al., 2004 investigated that TiO_2 nanoparticles can be obtained by using microemulsion methods. In this process the microemulsion of the precursor and the microemulasion precipitating agents are mixed by mixing two microemulsions. It can also be obtained by simple adding the precipitating agent to the microemulsion of the precursor. The method is very alike to the reaction used in sol gel method and both anatase and rutile polymorphs can be synthesized with microemulsion.

Other than that, according to Nakaso et al., (2003), gas phase synthesis is another important way for synthesise of TiO_2 particles. There are lots of studies investigating the formation of TiO_2 nanoparticles films in gas phase which are, chemical vapour deposition (CVD), physical vapour deposition (PVD), inert gas condensation, pulsed laser ablation spark discharge generation, ion sputtering, spray pyrolysis, laser pyrolysis/photothermal synthesis, thermal plasma synthesis, flame and flame spray pyrolysis techniques (Kim et al., 2004).

CHAPTER 3

METHODOLOGY

3.1 Materials

In this study, Titatinum-tetra-isopropoxide ($Ti(OC_3H_7)_4$) was used as a titanium source for the preparation of titania particles. While Aluminium isopropoxide ($Al(OC_3H_7)_3$) was used as aluminium source to prepare aluminium oxide particle. Ethanol is used as a solvent for both precursors. Sulphuric acid (H_2SO_4) was acted as a peptization agent to form a gel form in sol gel method. Distilled water was acted as a cleaner to remove the impurities.

3.1 Experimental Procedure

There are two steps in the methodology of proposed research. They are:

1) Preparation of Al_2O_3-TiO_2 and pure TiO_2 by using two methods which are sol gel method and hydrothermal method.
2) Characterization of the prepared catalyst by using Brunauer-Emmett-Tellar (BET) method, Fourier Transform Infrared Spectroscopy (FTIR), Scanning Electron Microscope (SEM), and X-Ray diffraction (XRD) .

3.2 Preparation of Al_2O_3-TiO_2 solution

Al_2O_3-TiO_2 solution was prepared as shown in Figure 3.1. From Figure 3.1, 3 g of $Al(OC_3H_7)_3$ was mixed with 50 mL of ethanol and 50 mL of water then stirred vigorously for 30 minutes by using magnetic stirrer. Meanwhile, 9 mL of

$Ti(OC_3H_7)_4$ and 41 mL of ethanol are mixed to produced $Ti(OC_3H_7)_4$ solution and stirred for 30 minutes. Under vigorous stirring the $Ti(OC_3H_7)_4$ solution was added drop by drop to $Al(OC_3H_7)_3$ solution and stirred for 4 hours. The same procedure was applied to produce pure TiO_2 without adding $Al(OC_3H_7)_3$.

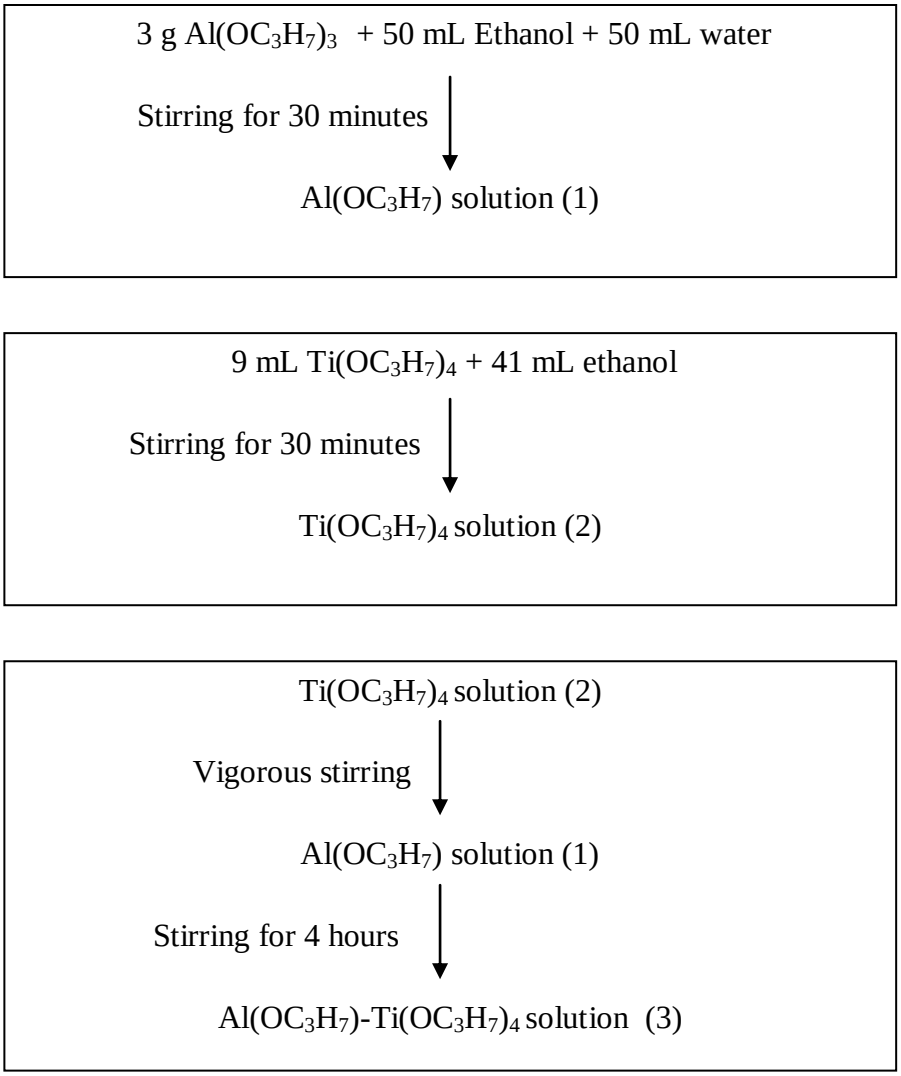

Figure 3.1: Formation of $Al(OC_3H_7)$-$Ti(OC_3H_7)_4$ solution

3.4 Sol Gel Method

In sol gel method as shown as in Figure 3.2, 1 M of sulphuric acid was added to $Al(OC_3H_7)_3$-$Ti(OC_3H_7)_4$ solution until the pH value of the solution approached 3. Then, the solution was heated at constant temperature at 70 °C by using double boiler method. The reaction was maintained until the gel was formed and ageing for 12 hours at room

temperature. The obtained white gel solution was filtered, washed several time with distilled water and dried at 102 ℃ for 2 hours in an oven to obtain the Al_2O_3-TiO_2 gel powder. The dried powder was grinded into small particles by using a mortar, and then calcined in a furnace at 500 ℃ for 2 hours to burn off the hydrocarbon. The obtained crystalline sol gel of Al_2O_3-TiO_2 powder was cooled down to room temperature, then transferred to a vial bottle. The procedure was repeated to produce pure TiO_2 powder.

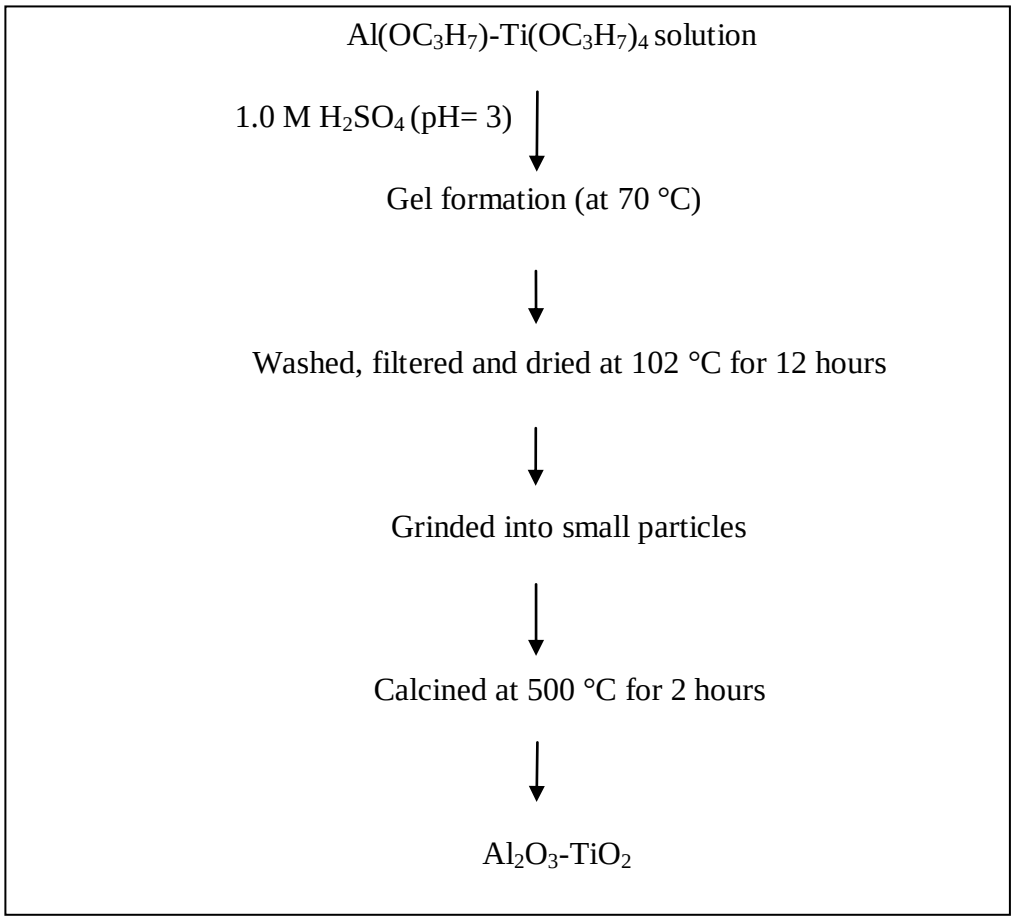

Figure 3.2: Formation of Al_2O_3-TiO_2 by using sol gel method

3.5 Hydrothermal Method

Figure 3.3 shows the steps in hydrothermal method. The prepared $Al(OC_3H_7)_3$-$Ti(OC_3H_7)_4$ solution in a beaker was tightly sealed by using aluminium foil. Then, transferred to an autoclave model H+P Varioklav Dampfsterilisator which heated at 121 °C under 2 bar for 2 hours. The sterilised $Al(OC_3H_7)_3$-$Ti(OC_3H_7)_4$ solution was ageing for 12 hours at room temperature. The solid and liquid particles of $Al(OC_3H_7)_3$-

$Ti(OC_3H_7)_4$ solution was separated in a centrifuge at 10000 rpm for 10 minutes and washed with distilled water. The separated solid particle was dried at 102 °C for 12 hours in oven and followed by calcination in furnace at 500 °C for 2 hours. The calcined Al_2O_3-TiO_2 powder was transferred into a vial bottle. The procedure was repeated to produce pure TiO_2 powder.

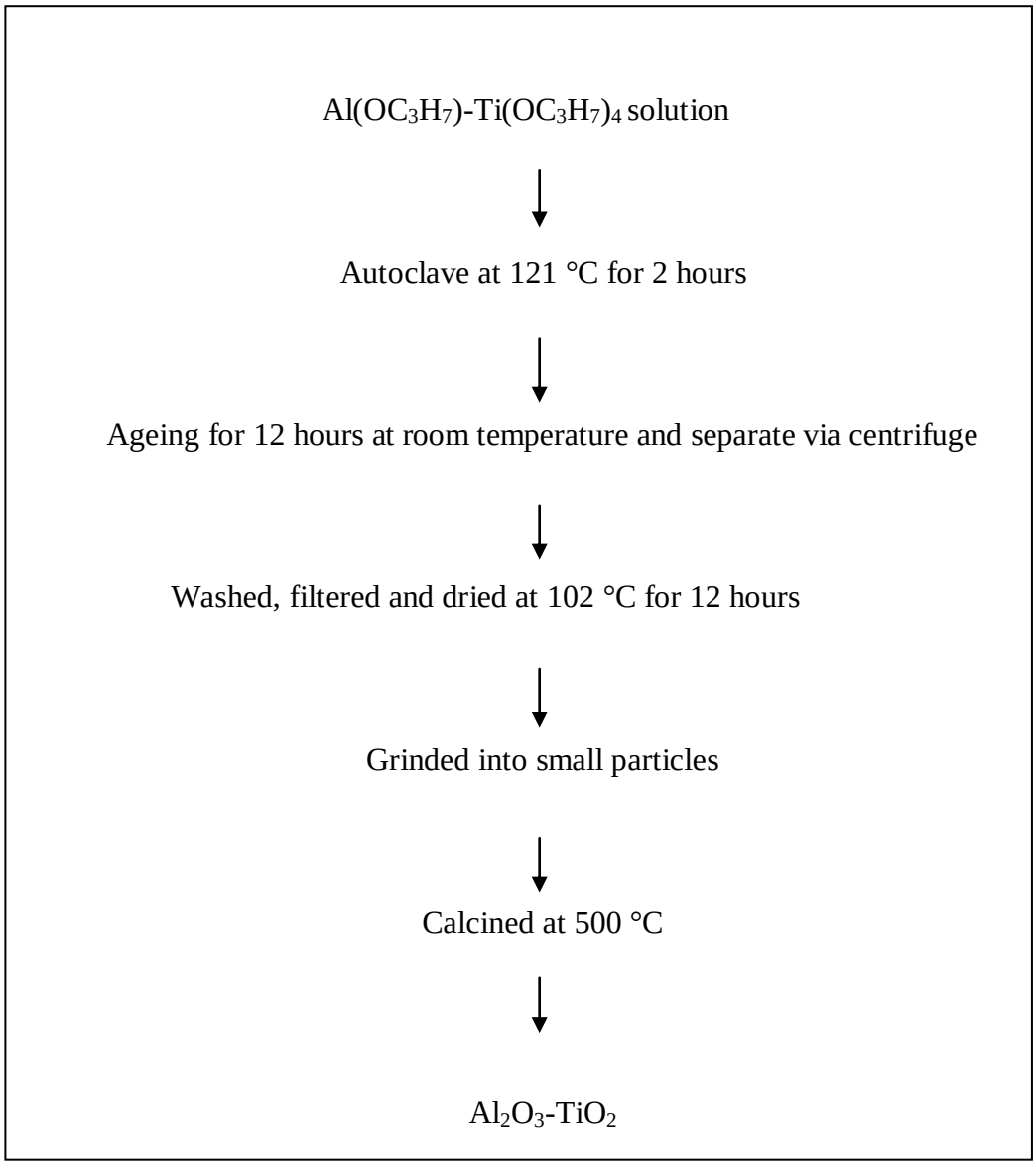

Figure 3.3: Formation of Al_2O_3-TiO_2 by using hydrothermal method

3.6 Characterization of the prepared catalyst

3.6.1 Surface morphology with Scanning Electron Microscope (SEM)

SEM was used to observe and study the difference of surface morphology between the Al_2O_3-TiO_2 and pure TiO_2 catalysts powder. The scanning of Al_2O_3-TiO_2 and pure TiO_2 catalysts powder images were carried out in the 30-2000 X magnificent range by using Zeiss Supra 55 Ultra SEM that enables to unsurpassed performance at beam energies from 100 V to 8 kV.

3.6.2 Identifying the functional group with Fourier Transform Infrared Spectroscopy (FTIR)

FTIR was used to study and identifying the types of functional group in the prepared catalysts. FTIR studies of Al_2O_3-TiO_2 and pure TiO_2 catalysts powder were carried out in the 400-4000 cm^{-1} frequency range in the transmission mode by using Nicolet Avatar 370 DTGS smart diffuse reflectance.

3.6.3 Crystalline phase characterization with X-Ray Powder Diffraction (XRD)

It was used to determine the crystalline phase of Al_2O_3-TiO_2 and pure TiO_2 catalysts powder. The XRD patterns were obtained from a Rigaku D/Max 2500 VB2+/PC diffractometer using Nickel filtered CuK. Radiation (λ=0.154184 nm) that operated at 40 kV and 30 mA. The scanning range was 23-63 with a step size of 0.01 and a time per step of 1.0 s.

3.6.4 Surface area characterization with Brunauer-Emmett-Teller (BET)

BET was used to measure the specific surface area of the prepared catalysts. The surface areas of the Al_2O_3-TiO_2 and pure TiO_2 powder were determined by nitrogen adsorption at −196 °C using a Micromeritics ASAP 2020

physisorption analyzer. The samples were degassed at 300 °C for 6 hours prior to nitrogen adsorption measurements.

3.7 Research design

The most important key concept which involved in this research was a research design. It can be thought of as an appropriate procedure or guideline for conducting this research under certain conditions so that the all the objectives of this research can be achieved. The summary of the research design for this study was shown as in Figure 3.4 below:

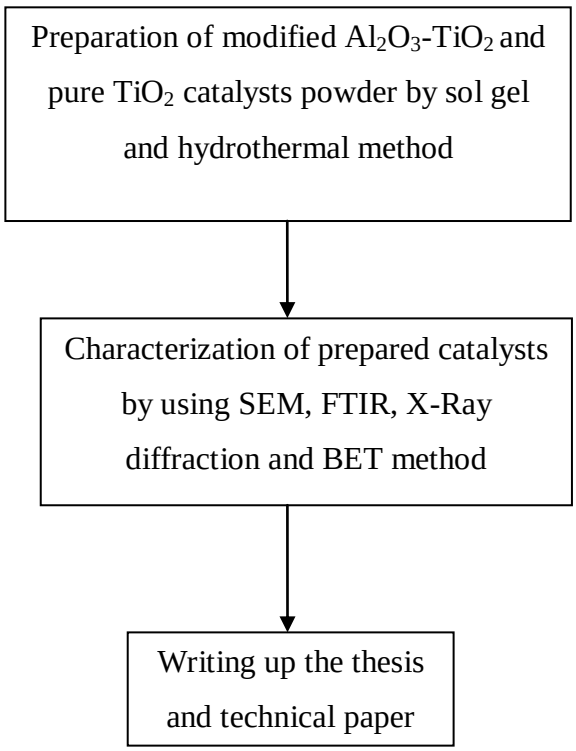

Figure 3.4: Research flow diagram of modified Al_2O_3-TiO_2

CHAPTER 4

RESULTS AND DISCUSSION

In this chapter, all the collected data obtained was further discussed based on the preparation of both Al_2O_3-TiO_2 and pure TiO_2**.** The properties of the prepared catalysts had been characterized by using SEM, FTIR, XRD and BET analysis.

4.1 SEM Analysis

In order to investigate the morphology of the prepared samples, comparison between the SEM images of the doped and un-doped TiO_2 had been studied. Figure 4.1(a) and 4.1(b) shows the comparison of surface morphology for pure TiO_2 and Al_2O_3-TiO_2 catalyst powder prepared by sol gel method. From Figure 4.1(a), the structure of pure TiO_2 shows a crystalline surface with a little aggregate. While in Figure 4.1(b), SEM analysis shows the deposition of particles on the surface of TiO_2 catalyst. However there is no significant effect on the aggregate sizes.

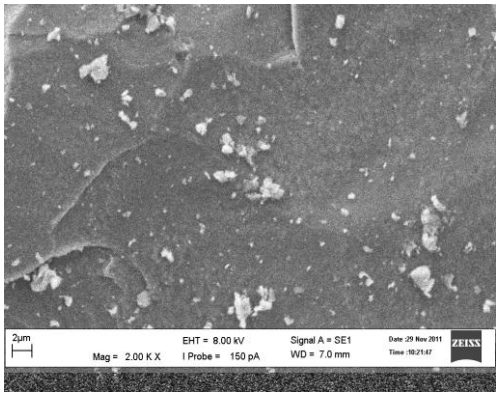

(a)

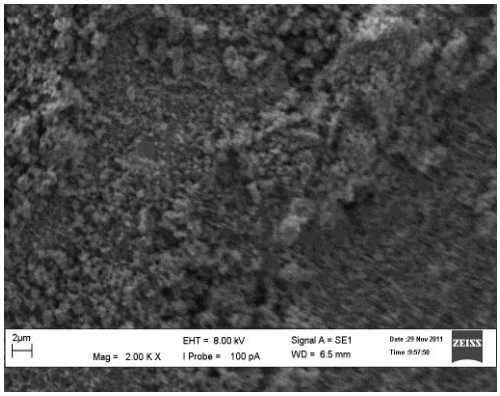

(b)

Figure 4.1: SEM analysis of the prepared catalysts by using sol gel method

(a) Pure TiO_2 (b) Al_2O_3-TiO_2

Meanwhile Figure 4.2(a) and 4.2(b) also shows the difference of the surface morphology of the prepared pure TiO_2 and Al_2O_3-TiO_2 catalyst by using hydrothermal method. From Figure 4.2(a), the surface of pure TiO_2 in the absence of Al_2O_3 has a crack but when Al_2O_3 was doped into TiO_2, the surface morphology of the catalyst exhibits well arranged aggregates with many small spherical particles as shown in Figure 4.2(b).

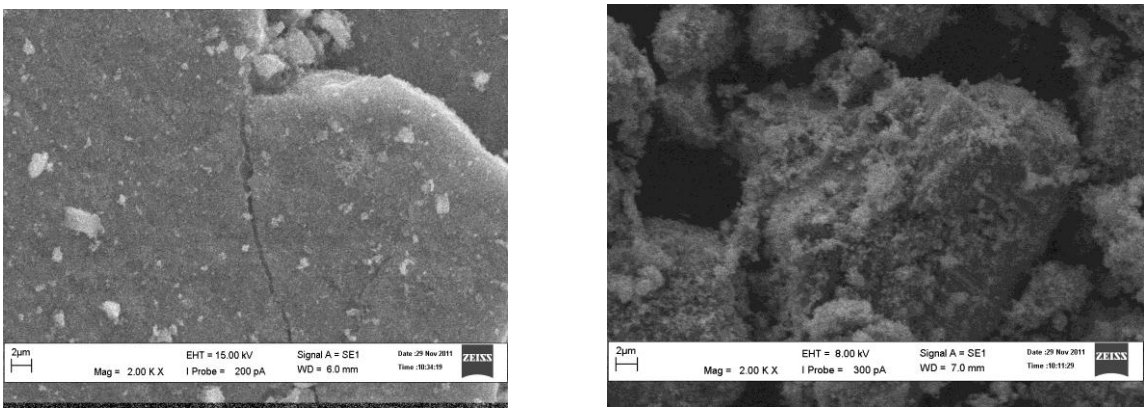

(a) (b)

Figure 4.2: SEM analysis of the prepared catalysts by using hydrothermal method (a) Pure TiO_2 (b) Al_2O_3-TiO_2

4.2 FTIR Analysis

In this study of FTIR analysis was used to collects spectral data in a wide spectral range which measures the intensity over a narrow range of wavelengths at a time. FTIR is most useful analysis for identifying chemicals that are either organic or inorganic. It can be utilized to quantify some components of an unknown mixture. The comparison of types of functional groups by using sol gel and hydrothermal had been investigated. The spectral data result for pure TiO_2 prepared by using sol gel method was illustrated in Figure 4.3 (a). From Figure 4.3(a), the % transmittance of pure TiO_2 begins at 43 % of infrared absorptions and there are three main peaks obtained which are at 3374.45 cm^{-1}, 1645.04 cm^{-1} and 917.01 cm^{-1}.

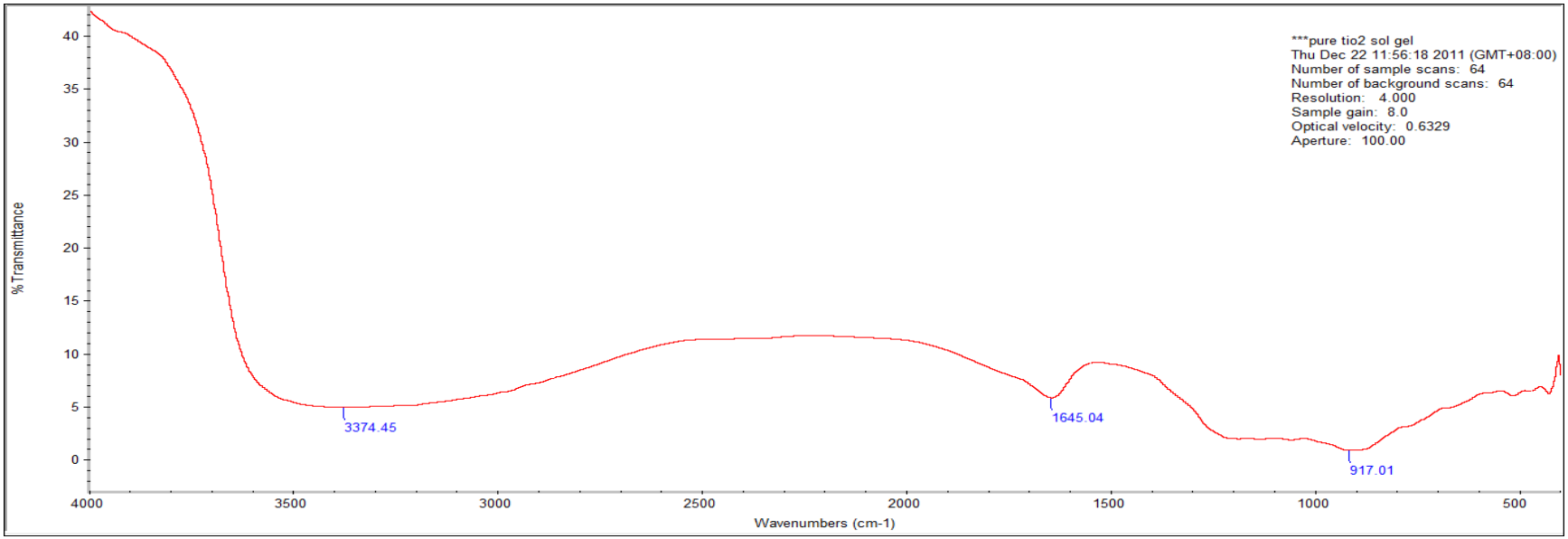

Figure 4.3 (a): FTIR analysis of Pure TiO_2 catalysts using sol gel method

Meanwhile, spectral data result for Al_2O_3-TiO_2 prepared by using sol gel method is shown in Figure 4.3(b). From the obtained result, it shows that when Al_2O_3 was doped in TiO_2 particles, the % transmittance of the spectral had increased from 40 % to 75 % of infrared absorptions. The observed peaks present in modified Al_2O_3-TiO_2 also changed. There are more peaks obtained in modified Al_2O_3-TiO_2 than in pure TiO_2. The observed peaks are at 3325.34 cm^{-1}, 2346.84 cm^{-1}, 1641.90 cm^{-1} and 1234.57 cm^{-1}.

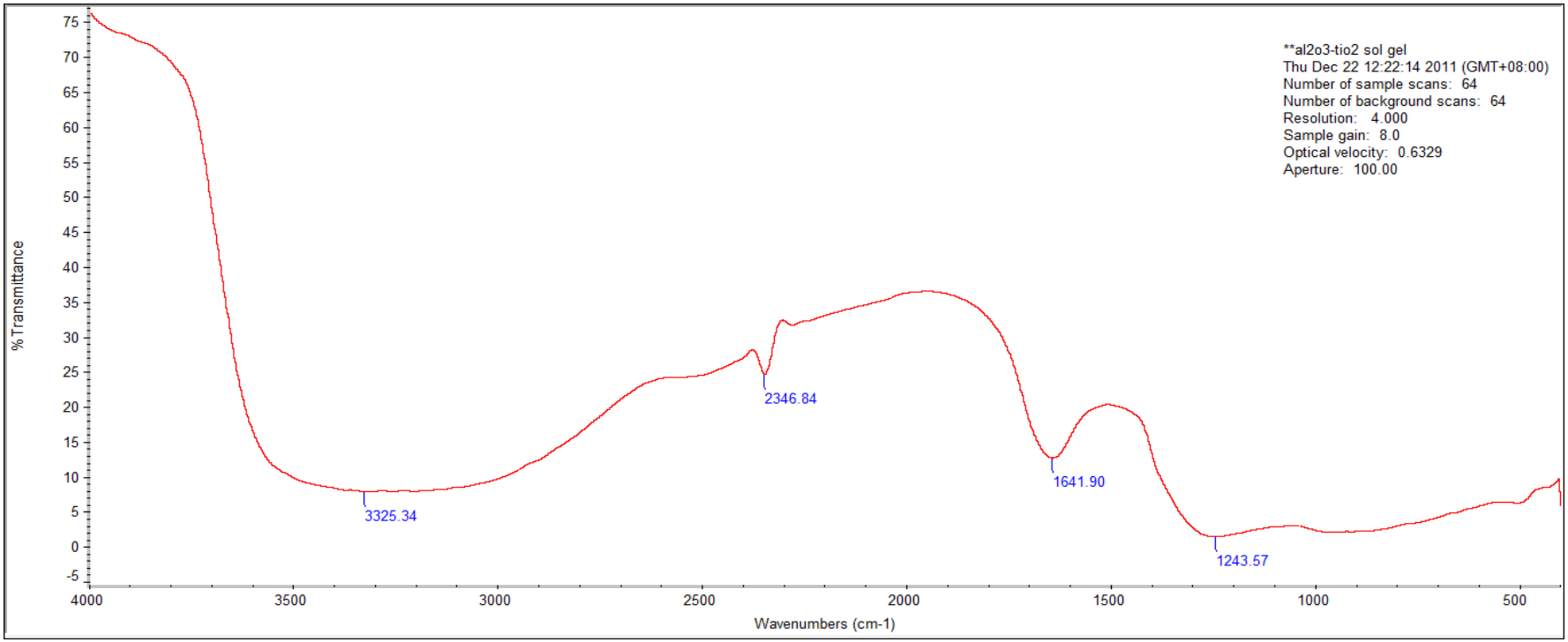

Figure 4.3 (b): FTIR analysis of Al_2O_3-TiO_2 catalysts using sol gel method

Both spectral of the prepared catalysts by using sol gel methods are correspond to inorganic nitrates and aliphatic primary amides. Inorganic nitrates peaks of 1645 cm^{-1} found in pure TiO_2 have very characteristic spectra. There are three characteristic bands at around 1780 cm^{-1}, 1380 cm^{-1} and 830 cm^{-1}. If the peak occurs near 1380 cm^{-1} it will be the strongest bond and is relatively broad while the other two absorptions are weaker and very narrow. There may also be the typical water bands around 3400 cm^{-1} and 1640 cm^{-1}. Meanwhile, in Al_2O_3-TiO_2, peaks of 1641.90 cm^{-1} is present in the simple inorganic nitrites spectra. The spectra consist of two bonds which are a broad strong band around 1260 cm^{-1} and a very sharp, medium intensity band around 825 cm^{-1}. According to Fisher et al., (2004), the general region of the Al-O vibrations of Al_2O_3 spectra is in range 950-800 cm^{-1}. The strong peak is at 855 cm^{-1} which will clearly indicates the formation of Al-O bond. However, in this research, the existence of Al-O bonds in the Al_2O_3-TiO_2 powder catalysts was unable to be observed. Alternatively, the Al-H bonds may form but may be oriented parallel to the surface, thereby diminishing the IR intensity (Fisher et al., 2004).

Meanwhile for the prepared samples by using hydrothermal method are illustrated in Figure 4.4. Figure 4.4(a) shows the spectral results of pure TiO_2. From Figure 4.4(a), the % transmittance of pure TiO_2 begins at 95 % of infrared absorptions and there are three main peaks obtained which are at 3339.02 cm^{-1}, 1638.94 cm^{-1} and 933.31 cm^{-1}.

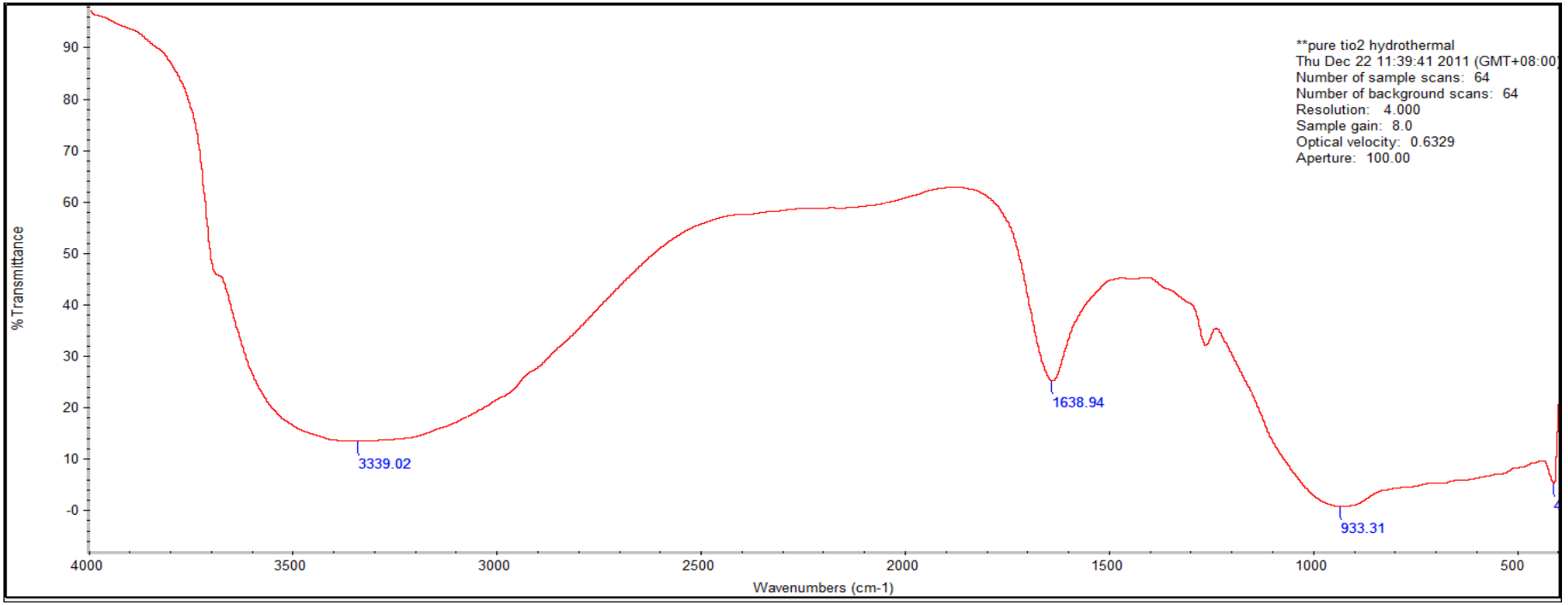

Figure 4.4 (a): FTIR analysis of pure TiO_2 catalysts using hydrothermal method

While, spectral data result for modified Al_2O_3-TiO_2 prepared by using sol gel method was shown in Figure 4.4(b). From the result, it shows that there is no significant change in the % transmittance when Al_2O_3 was doped in TiO_2 particles. There are three observed peaks present in Al_2O_3-TiO_2 which are at 3401.85cm^{-1}, 1640.12 cm^{-1} and 947.75 cm^{-1}. In hydrothermal methods, the presence of Al-O bonds in the TiO_2 powder was successfully obtained as the peaks of 947.75 cm^{-1} fall in the general range of Al-O vibrations. The spectral results in both the prepared catalysts in hydrothermal methods are corresponds to aliphatic primary amides. According to Barry (1991), amides have quite high boiling points because they are capable of strong intermolecular interactions. This is due to the present of various types of stretch present in amides group.

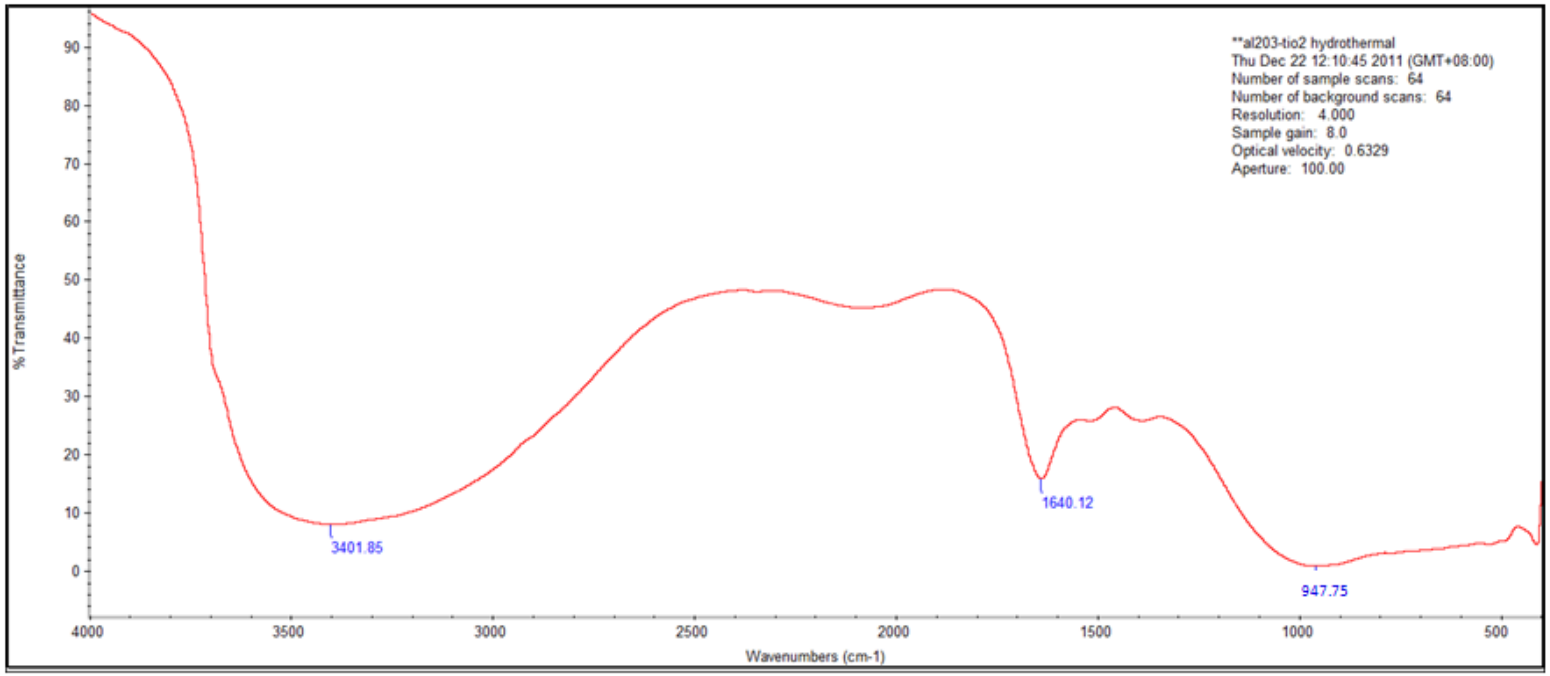

Figure 4.4 (b): FTIR analysis of Al_2O_3-TiO_2 catalysts using hydrothermal method

There four main stretches present in aliphatic amide groups which are NH stretching, CO (amide I), NH_2 (amide II) and Amide (III). The details of each stretch are shown in Table 4.1.

Table 4.1: Summary of the spectral interpretation in Aliphatic Amide Group

Types of Stretch	Details
NH Stretching	Primary: Near 3350-3180 cm^{-1} Secondary: 3320-3070 cm^{-1} (trans and cis)
CO (amide I)	Primary: Near 1650 cm^{-1} Secondary: 1680-1630 cm^{-1} Tertiary 1670-1630 cm^{-1}
NH_2 (amide II)	Primary: 1650-1620 cm^{-1} Secondary: 1570-1515 cm^{-1}
Amide III	Secondary: Near 1270 cm^{-1}

In this research the summary of the analyzed peaks found are shown in Table 4.2. From Table 4.2, it shows that the aliphatic primary amide group is the main functional group that was present in all the prepared catalysts. Meanwhile inorganic nitrites only present in the prepared samples by using sol gel method.

Table 4.2: Presences of functional groups in the prepared catalysts using FTIR analysis

Catalyst	Peaks found (wavenumber, cm^{-1})	Groups present
Pure TiO_2 (sol gel)	3374.45, 1645.04 and 917.01	• Aliphatic primary amides • Inorganic nitrites
Al_2O_3-TiO_2 (sol gel)	3325.34, 2346.84, 1641.90 and 1243.57	• Aliphatic primary amides • Inorganic nitrites
Pure TiO_2 (hydrothermal)	3339.02, 1638.94 and 933.31	• Aliphatic primary amides
Al_2O_3-TiO_2 (hydrothermal)	3401.85, 1640.12 and 947.75	• Aliphatic primary amides

The summary of comparison of spectral data result for all the prepared samples in both sol gel and hydrothermal method is shown in Figure 4.5.

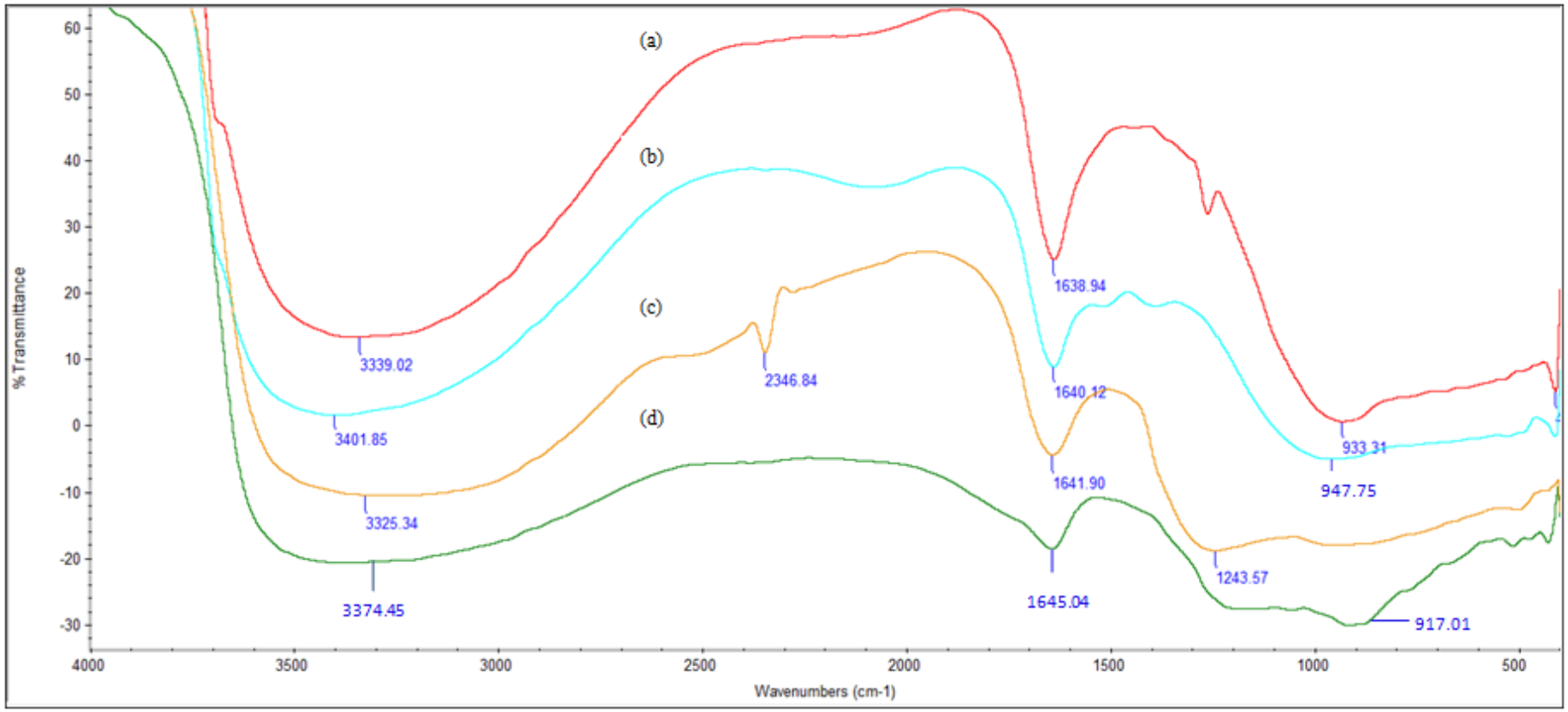

Figure 4.5: Comparison of FTIR analysis of the prepared catalysts (a) Pure TiO_2 (hydrothermal) (b) Al_2O_3-TiO_2 (hydrothermal) (c) Pure TiO_2 (sol gel) (d) Al_2O_3-TiO_2 (sol gel)

4.3 XRD analysis

XRD analysis was conducted to investigate and to determine the crystalline phase of pure TiO_2 and Al_2O_3-TiO_2 catalysts powder. XRD patterns of pure TiO_2 and Al_2O_3-TiO_2 prepared by using sol gel method were illustrated in Figure 4.6. From Figure 4.6(a), XRD analysis revealed that the highest peak is at 2Θ= 25.280 ° with 1062 cps of intensity. Follow by a peak with 302 cps of intensity which present at 2Θ= 47.960 ° and the lowest peak is with 242 cps of intensity at 2Θ= 38.020 °. Based on XRD analysis, all the peaks in pure TiO_2 exhibit the anatase of TiO_2 phase. The summary data for pure TiO_2 prepared by sol gel method was shown in Table 4.3.

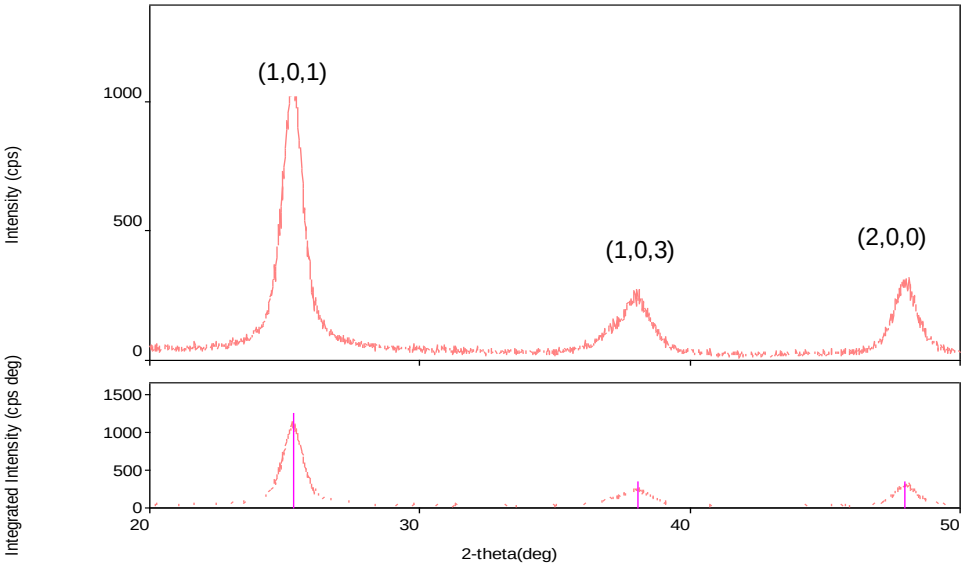

Figure 4.6 (a): XRD pattern of the Pure TiO_2 catalyst by using sol gel method

Table 4.3: XRD analysis data of the pure TiO_2 catalyst by using sol gel method

2theta /2Θ (°)	Intensity(cps)	Phase name
25.280	1062	Anatase (1,0,1)
38.020	242	Anatase (1,0,3)
47.960	302	Anatase (2,0,0)

While in Al_2O_3-TiO_2 catalyst, the intensity of Al_2O_3-TiO_2 had changed drastically when Al_2O_3 was doped in TiO_2 particles. From Figure 4.6(b), there are only one peak revealed at 2Θ=25.680 ° with 265 cps of intensity. The intensity of doped TiO_2 is smaller than un-doped TiO_2. The absence of crystalline anatase form of Ti is maybe due to the formation of amorphous structure of Al_2O_3-TiO_2. The changes of phase to amorphous structure might be due to the long heating process during the preparing process of the samples using sol gel method. The summary data for Al_2O_3-TiO_2 prepared by sol gel method was shown in Table 4.4.

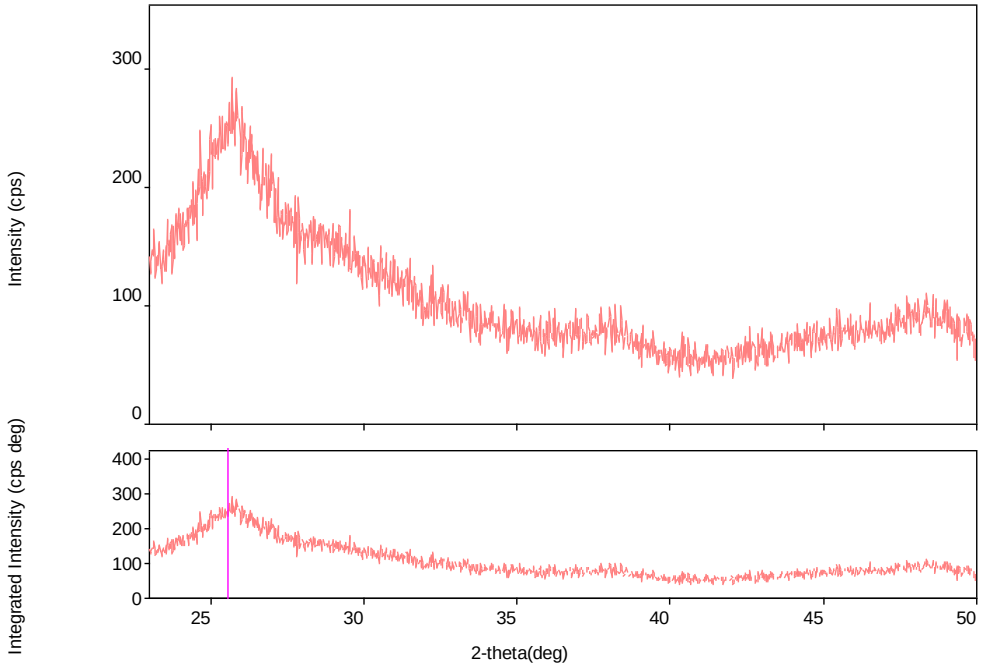

Figure 4.6 (b): XRD pattern of the Al_2O_3-TiO_2 catalyst by using sol gel method

Table 4.4: XRD analysis data of the Al_2O_3-TiO_2 catalyst by using sol gel method

2theta /2Θ (°)	Intensity	Phase name
25.680	265	Armorphous

Meanwhile in hydrothermal method, The XRD pattern of un-doped TiO_2 was shown in Figure 4.7(a). From Figure 4.7(a) the highest peaks of pure TiO_2 was revealed at 2Θ= 25.320 ° with 1391 cps of intensity. Follow by peak with 384 cps of intensity which present at 2Θ=48.080 ° and the lowest peak at 2Θ= 37.920 ° with 384 cps of intensity. All the peaks in pure TiO_2 which present in this method exhibit the anatase of TiO_2 phase. The summary data for pure TiO_2 prepared by hydrothermal method was shown in Table 4.5.

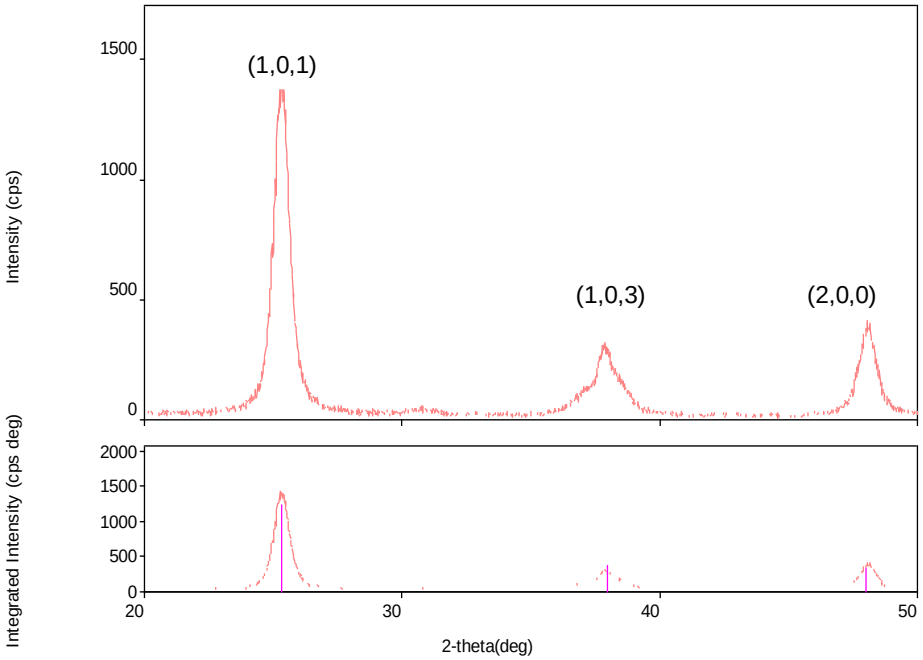

Figure 4.7 (a): XRD pattern of the pure TiO_2 catalyst by using hydrothermal method

Table 4.5: XRD analysis data of the pure TiO_2 catalyst by using hydrothermal method

2theta /2Θ (°)	Intensity	Phase name
25.320	1391	Anatase (1,0,1)
37.920	293	Anatase (1,0,3)
48.080	384	Anatase (2,0,0)

While in Al_2O_3-TiO_2 catalyst, the presence of Al_2O_3 particles in TiO_2 surface does not show a significant difference between the diffraction peaks but the value of intensity was decreased when Al_2O_3 was doped in TiO_2. From Figure 4.7(b), it shows the highest peak present at 2Θ= 25.320 ° with 1118 cps of intensity. Follow by peak at 2Θ= 48.040 ° with 313 cps of intensity and the lowest peak present at 2Θ= 38.000 ° with 254 cps of intensity. The crystalline phase of Al_2O_3-TiO_2 catalyst is similar to pure TiO_2 which show anatase phase. The summary data for Al_2O_3-TiO_2 catalyst prepared by hydrothermal method is shown in Table 4.6.

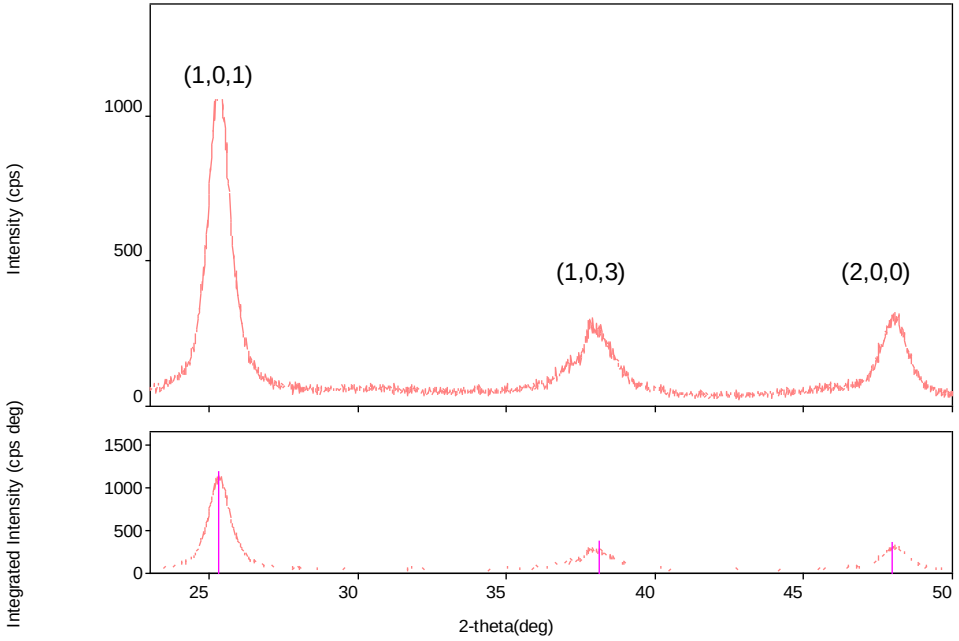

Figure 4.7 (b): XRD pattern of the Al_2O_3-TiO_2 catalyst by using hydrothermal method

Table 4.6: XRD analysis data of the Al_2O_3-TiO_2 catalyst by using hydrothermal method

2theta /2Θ (°)	Intensity	Phase name
25.320	1118	Anatase (1,0,1)
38.000	254	Anatase (1,0,3)
48.040	313	Anatase (2,0,0)

The comparison of XRD pattern for all the prepared catalysts was shown in Table 4.7. From Table 4.7 the pattern can be indexed to TiO_2 in the anatase phase only. The rutile and brookite phases of TiO_2 were not observed. This result indicates that all the prepared samples were successfully crystallized to be in anatase phase at the calcinations temperature at 500 °C except for Al_2O_3-TiO_2 catalyst prepared by sol gel method which exhibits amorphous structure of Al_2O_3-TiO_2. It is clear that the crystalline of anatase phase or crystal growth is favoured by hydrothermal treatment. According to Qui (2006), anatase phase is the most stable phase of TiO_2 due to the highly surface responsible for photocatalytic reaction that readily formed in the anatase structure. Thus, it exhibited great photocatalytic properties which will be useful to be use in the photoreduction process.

Table 4.7: Summary of XRD analysis for all the prepared catalysts

Sample	2-Theta (degree)	Phase name
Pure TiO_2 (sol gel)	25.306	Anatase
	38.05	Anatase
	47.94	Anatase
Al_2O_3-TiO_2 (sol gel)	25.54	Amorphous
Pure TiO_2 (hydrothermal)	25.321	Anatase
	37.97	Anatase
	47.982	Anatase
Al_2O_3-TiO_2 (hydrothermal)	25.293	Anatase
	38.09	Anatase
	47.97	Anatase

4.4 BET analysis

BET analysis was performed as an alternative method to measure the specific surface area and the pore size of the prepared catalysts. Specific surface area is one of the important parameter to enhance the photocatalytic properties. The ranges of specific area can widely depending upon the particle's size, shape and porosity of the sample (Lowell and Shields, 1998). From BET analysis, the specific area, adsorption isotherm and the pore size had been investigated. From BET analysis, there are obvious differences in the shapes obtained in the prepared catalysts using sol gel and hydrothermal method.

In terms of specific surface area, the modified Al_2O_3-TiO_2 powder catalyst prepared by hydrothermal methods shows the highest surface area than the other prepared samples with 153.8599 m^2/g of surface area. Followed by pure TiO_2 prepared by sol gel method with 112.2804 m^2/g of surface area, pure TiO_2 prepared by hydrothermal method with 81.3916 m^2/g of surface area and lastly is the Al_2O_3-TiO_2 prepared by sol gel method with 27.0919 m^2/g of surface area. The specific surface area for each sample is shown in Table 4.8.

Table 4.8: The BET specific surface areas of the pure TiO_2 and Al_2O_3-TiO_2

Sample	Surface Area (m^2/g)
Pure TiO_2 (sol gel)	112.2804
Al_2O_3-TiO_2 (sol gel)	27.0919
Pure TiO_2 (hydrothermal)	81.3916
Al_2O_3-TiO_2 (hydrothermal)	153.8599

In photoreduction process, the ability of the catalysts to absorb the UV light depends on pore size which is the key to have great photoinduced properties of TiO_2. The determination of pore size is related to BET adsorption isotherm analysis and the pore size distribution plots. According to Brunauer et al., (1940), adsorption isotherm is a measurement of the amount of gas adsorbed over a range of partial pressures at single temperature results. During the N_2 adsorption process, the gas will comes into contact with the surface of the catalyst, and adsorb to the surface in quantities that are a function of their partial pressure in the bulk. Essentially there are five different types of isotherms that are obtained for the adsorption of gases on solids which are type I, II, III, IV and V.

In the other hand, for pore size, there are three types which are microporous, macroporous and mesoporous material (Lowell and Shields, 1998). According to IUPAC notation, particles which have less than 2 nm of pore diameter are categories as microporous materials. For the particles which have a greater pore diameter than 50 nm are called macroporous material. Lastly, is the mesoporous category which lies in the middle of microporous and macroporous range (Lowell and Shields, 1998).

Figure 4.8 and 4.9 shows the analysis for pure TiO_2 prepared by using sol gel method. Based on Figure 4.8, the type adsorption isotherm of pure TiO_2 is type IV hysteresis loop. While from Figure 4.9, the pore size diameter of pure TiO_2 was revealed to have around ~9.3 nm.

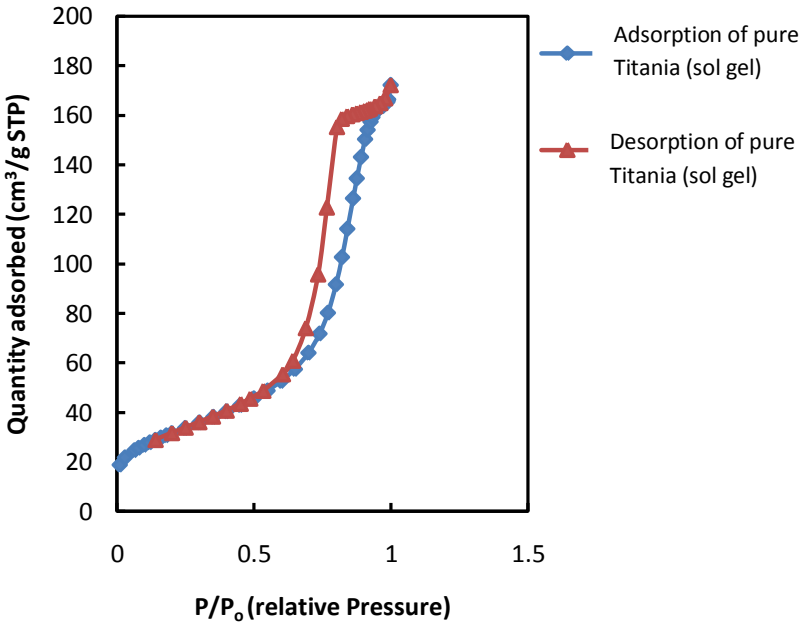

Figure 4.8: N_2 adsorption desorption isotherm of pure TiO_2 by using sol gel method

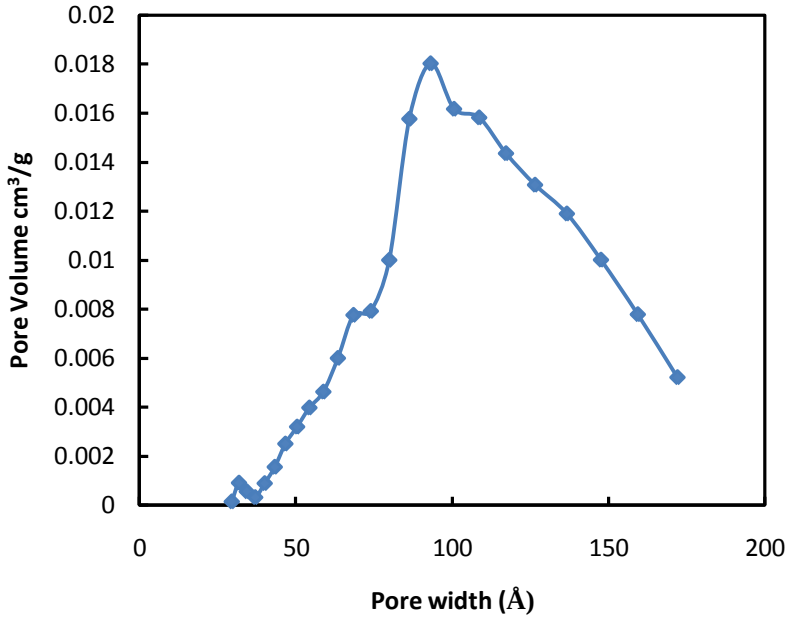

Figure 4.9: Pore size distribution of pure TiO_2 using sol gel method

Figure 4.10 and 4.11 shows the analysis for Al_2O_3-TiO_2 prepared by using sol gel method. Based on Figure 4.10, the type adsorption isotherm of Al_2O_3-TiO_2 is type IV hysteresis loop. While from Figure 4.11, the pore size diameter of Al_2O_3-TiO_2 was revealed to have around ~9.4 nm.

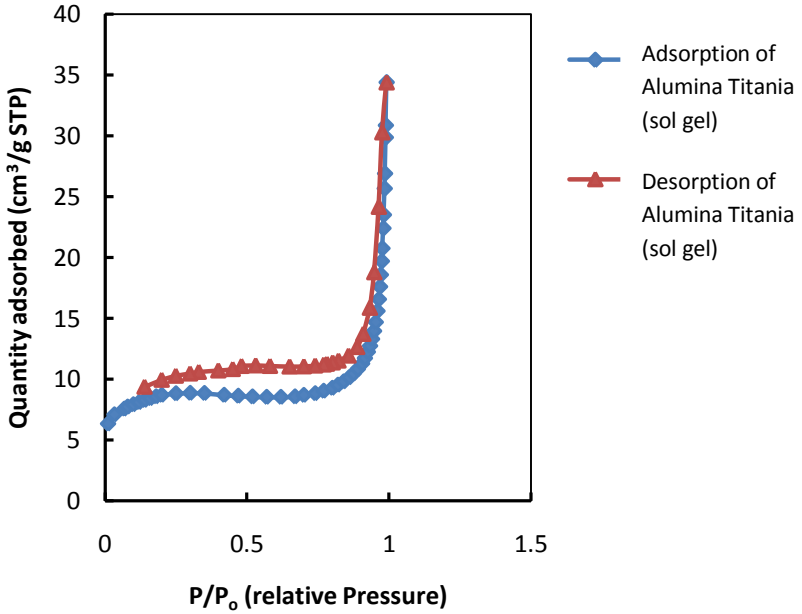

Figure 4.10: N_2 adsorption desorption isotherm of Al_2O_3-TiO_2 by using sol gel method

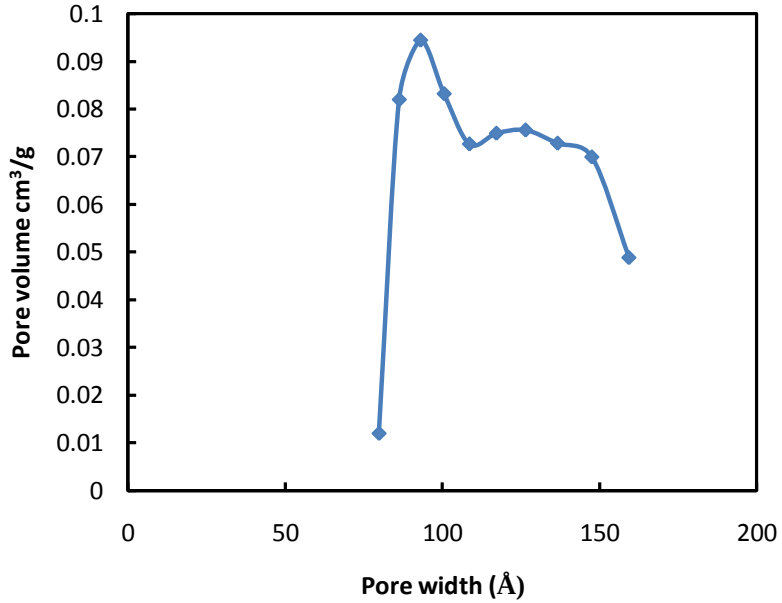

Figure 4.11: Pore size distribution of Al_2O_3-TiO_2 using sol gel method

Figure 4.12 and 4.13 shows the analysis for pure TiO_2 prepared by using hydrothermal method. Based on Figure 4.12, the type adsorption isotherm of pure TiO_2 is type IV hysteresis loop. While from Figure 4.13, the pore size diameter of pure TiO_2 was revealed to have around ~9.3 nm.

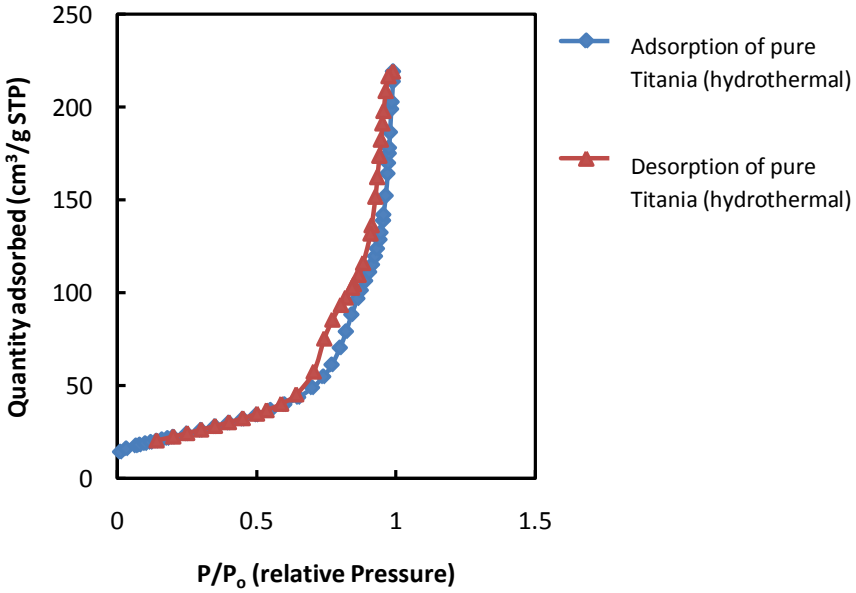

Figure 4.12: N_2 adsorption desorption isotherm of pure TiO_2 by using hydrothermal method

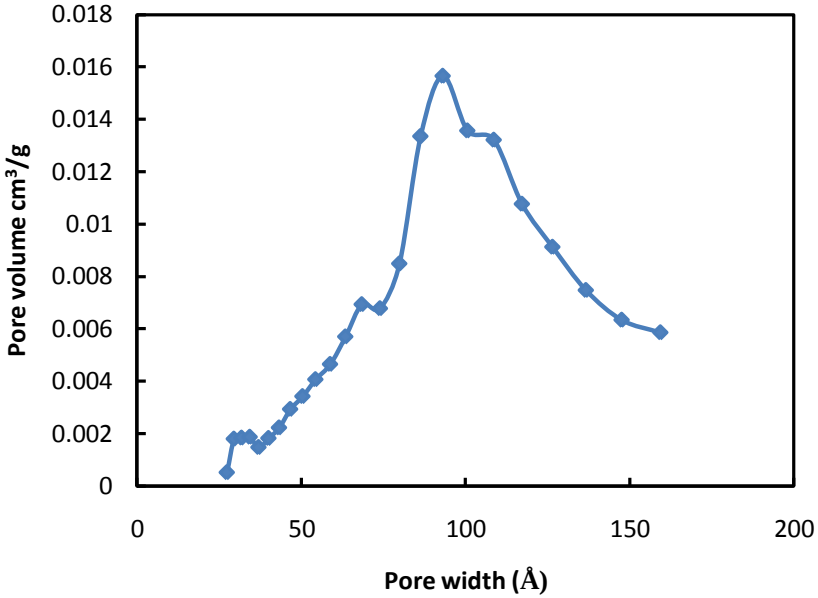

Figure 4.13: Pore size distribution of pure TiO_2 using hydrothermal method

Figure 4.14 and 4.15 shows the analysis for Al_2O_3-TiO_2 prepared by using hydrothermal method. Based on Figure 4.14, the type adsorption isotherm of Al_2O_3-TiO_2 is type IV hysteresis loop. While from Figure 4.15, the pore size diameter of Al_2O_3-TiO_2 was revealed to have around ~8.8 nm.

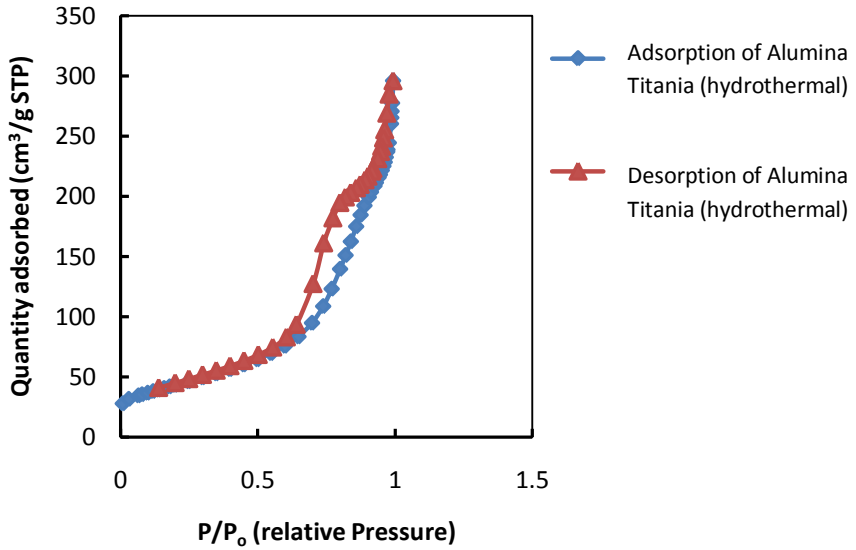

Figure 4.14: N_2 adsorption desorption isotherm of Al_2O_3-TiO_2 by using hydrothermal method

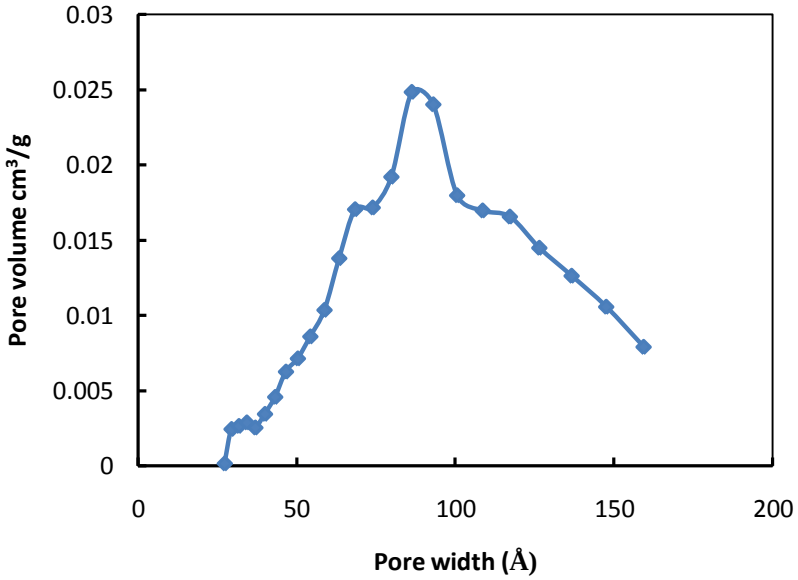

Figure 4.15: Pore size distribution of Al_2O_3-TiO_2 using hydrothermal method

The mean pore size of all samples was around ~ 8.8-9.4 nm, the pore size distribution being relatively narrows. From this research all the prepared samples have a type IV of adsorption isotherm. It was characterize of mesoporous absorbent with strong and weak affinities, respectively. Other than that, it also shows adsorption hysteresis at lower temperature. At lower pressure region of graph type IV is quite similar to type II that at high relative pressures the isotherm appears to reach a saturation value or increases asymptotically which explains the formation of monolayer adsorption region followed by multilayer adsorption region (Katsumi, 1994).

In this research the objective to produce nanoporous catalysts which have a specifically high surface area, small porosity and of course very ordered, uniform pore structure had been achieved. According to Murray et al., (2009), nanoporous catalysts have very versatile and rich surface composition, surface properties, which can be used for functional in increasing the photocatalytic activity of TiO_2. Moreover, the surface defects can act as a hole trapping centers in the photocatalysis process. With the decreasing in size, the surface to volume ratio is increases and the surface effect become more active and TiO_2 nanoparticles with a high surface volume ratio can be obtained (Murray et al., 2000).

From this research, it can be seen that the products were strongly dependent on the preparing methods as the results vary with different methods. From the analysis results, hydrothermal method is best method to be used to produce the Al_2O_3-TiO_2 than a sol gel method as the characteristics of the samples produce enhanced the photocatalysis properties. The main key in this research is the crystal growth of the prepared samples. In particular, crystal growth can be vital in controlling the phase, shape, and size of photocatalysts, together with their crystallinity and surface area. By rationally controlling crystal growth, the intrinsic surface atomic structure and resultant surface states of the derived photocatalysts can be tailored (Gang et al., 2009).

In hydrothermal method, the crystal growth progressed smoothly as it gave a positive change in the photocatalytic activity. In this method, the surface area of the pure TiO_2 was increased when it is doped with Al_2O_3. This result indicated that the addition of amorphous Al_2O_3 into TiO_2 matrix in hydrothermal method increased the

surface area and thus increases the surface adsorption of the Al_2O_3-TiO_2. Surface area and porosity are very important parameters that need to be considered for TiO_2 photocatalysts to acts as good catalysts. The surface area and pore volume shows the ability of the adsorptions of the particles. It will enhance the electron-hole pair separation which is the important parameter in considering the photocatalytic activity (Paola et al., 2004). Fewer recombination sites on the surface lead to slower recombination of electrons and holes, thus a higher photocatalytic activity.

Meanwhile, in this sol gel method the samples were prepared at pH 3 in acid media where the hydrolysis reaction is much faster than polycondensation and resulted the gels to be hydroxylated (Lopez et al., 1992). The dehydroxylation process (OH^-) initiates at around 200 °C and the subsequent dehydration of the solids generates singly ionized anionic vacancies. When the samples are synthesized using H_2SO_4 as the hydrolysis catalyst in the gelation reaction, they absorb at a lower energy than the samples prepared at basic hydrolysis catalysts. This is reflected in the band gap values and will help to enhance the photocatalytic activity of TiO_2 by reducing the band gap values (Sanchez and Lopez, 1995).

As reported previously, the TiO_2 catalyst powder prepared at pH 3 forms rutile at high temperature and anatase at low temperature (Lopez et al., 1992). In addition, previous research conducted by Kumar et al., (1992) also claimed that powder catalyst produced by sol gel method will give a catalyst with extremely high surface area. However, in this research the crystal growth of the Al_2O_3-TiO_2 could not be obtained. This might be due to the disturbance that perhaps occurs during the gelation process as it play the important roles in controlling the crystal growth process of the final products of Al_2O_3-TiO_2. Other than that, the time taken to complete the gelation process also might effects the properties of Al_2O_3-TiO_2. It demonstrated that doping of Al_2O_3 on TiO_2 particles does induce appreciable change in the surface area of pure TiO_2 as the surface area of the Al_2O_3-TiO_2 is smaller than the pure TiO_2 catalyst.

CHAPTER 5

CONCLUSION AND RECOMMENDATIONS

5.1 Conclusions

The aim of this study was to synthesize nanostructured of Al_2O_3-TiO_2 powder catalyst with better photocatalytic activity to be applied in the photoreduction process by using sol gel and hydrothermal method. For comparison, the same compositions of titanium and aluminium precursor were used in both methods. In this research, the effect of Al_2O_3 loading on TiO_2 was investigated. The synthesized samples were characterized by SEM, FTIR, XRD and BET.

Experimental results demonstrated that hydrothermal method was a promising technique for preparing Al_2O_3-TiO_2 photocatalysts as it fulfilled all the requirement properties to enhance the photocatalytic activity of TiO_2 in the photoreduction process. Based on SEM analysis, the surface morphology of Al_2O_3-TiO_2 catalyst exhibits well arranged aggregates with many small spherical particles. In addition, through FTIR analysis, the presence of Al-O bonds in the TiO_2 powder was successfully obtained as the peaks of 947.75 cm^{-1} fall in the general range of Al-O vibrations. Other than that, based on XRD pattern it revealed the existence of polymorphs anatase TiO_2 in Al_2O_3-TiO_2 catalyst which usually shows greatly superior in photoactivity of TiO_2. Most importantly, based on BET analysis, the prepared Al_2O_3-TiO_2 catalysts show a great crystal growth with 153.8599 m^2/g specific surface area and 8.8 nm of pore size diameter. A nano size material will lead to improvement in the electron hole pair separation and enhance the photoactivity of TiO_2.

5.2 Recommendations

For future improvements, in order to gain an ideal crystal growth which gives good electronic structures and surface transfer of photoinduced change carriers on the photoreduction process, the design of the configuration and the distribution of dopants (Al_2O_3) in TiO_2 particles should be further investigated. It is important to control the surface heteroatomic structure of TiO_2 to guarantee that photoinduced electrons and holes are powerful enough, under solar irradiation, to promote surface charge-carrier transfer for successive photoreduction. The recommendation to enhance the properties of the prepared catalysts can be divided into two parts which. Part one is about the preparation of the catalyst while the second part is about the characterization of the prepared catalyst.

5.2.1 Preparation of the catalyst

In terms of preparation of the catalyst, there should be various parameters that should be considered as it will affect the properties of the prepared catalyst. The duration of aging, the ratio of ethanol to water, calcination temperature, type of precursor used should be further investigated. In sol gel method, the variety parameters that should be tested are the pH value and gelation temperature. Meanwhile in hydrothermal, the important parameters are the duration and the temperature of hydrothermal treatment.

5.2.2 Characterization of the prepared catalyst

In terms of characterization, more equipment should be use to fully analyzed so that the characteristic of the prepared catalyst can be observed in details. For instance, Transmission Electron Microscopy (TEM) analysis should be perform instead of using SEM analysis as the results obtained from SEM are not clearly display the morphology of the catalysts. Besides that, in order to detect the composition and the presence of doped material, SEM attached with EDX should be used so that the catalyst can be fully examined.

In the other hand, to investigate and in order to obtain the complete results of the prepared catalyst, the photoactivity test should be conducted in photoreactor column so that the exact results for the prepared catalyst can be completely obtained. Thus, it can be apply in the photoreduction process.

REFERENCES

Akurati, K.K., Bhattacharya, S.S, Wintere, M. and Hahn, H. 2006. Synthesis, characterization and sintering of nanocrystalline titania powders produced by chemical vapour synthesis. *Journal of Physics D: Applied Physics*. **39**: 2248-2254.

Alp, Y. 2009. *The synthesis of Titanium Dioxide photocatalysts by sol gel method: the effect of hydrothermal method treatment conditions and use of carbon nanotube template.* Ph.D. Thesis. Middle East Technical University.

ALCOA. 1969. *Activated and Catalytic Aluminas*. Aluminum Company of America, Pittsburgh. 1-12.

Alexia, N., Stergiopoulosa, T., Kontosa, A.G., Tsouklerisa, D.S., Katsoulidisb, A.P., Pomonisb, P.J., Leclerec, D.J., Skeldonc, P., Thompsonc, G.E. and Falaras, P. (2009). Mesoporous titania nanocrystals prepared using hexadecylamine surfactant template: Crystallization progress monitoring, morphological characterization and application in dye-sensitized solar cells. *Microporous and mesoporous materials.***124**: 52-58.

Al-Salim, N.Y., Abagshaw, S., Bittar, A., Kemmett, T., McQuilla, A. J. and Mills, A.M., 2000. Characterisation and activity of sol gel prepared TiO_2 photocatalysts modified with Ca, Sr or Ba ion additives. *Journal of Materials Chemistry*. **10**: 2358-2363.

Aminian, M.K., Taghavinia, N., Iraji-zad, A. and Mahdavi, S.M. 2006 . Highly porous TiO_2 nanofibres with a fractal structure. *Nanotechnology*. **17**: 520-525.

Aprile, C., Corma, A. and Garcia, H. 2008. Enhancement of the photocatalytic activity of TiO_2 through spatial structuring and particle size control: from subnanometric to submillimetric length scale. *Physical Chemistry Chemical Physics*. **10**: 769-783.

Asahi, R., Morikawa, T., Ohwaki, T., Aoki, K. and Taga, Y. 2001. Visible-light photocatalysis in nitrogen-doped titanium dioxide. *Science*. **293:** 269-271.

Barry, M.T. 1991. *Comprehensive organic synthesis*: Selectivity, Strategy and efficiency in modern organic chemistry. **8**. UK: ELSEVIER Ltd

Bennania, J., Dillert, R., Gesing, T.M. and Bahnemanna, D. 2009. Physical properties, stability and photocatalytic activity of transparent TiO_2/SiO_2 films. Separation *and Purification Technology*. **67**: 173-179.

Borse, P.H., Kankate, L.S., Dassenoy, F., Vogel, W., Urban, J. and Kulkarni, S. K. 2002. Synthesis and investigations of rutile phase nanoparticles of TiO_2. *Journal of Material Science*. **13:** 553-559.

Bragg, L., Claringbull, G.F., and Taylor, W.H. 1965. *Crystal structures of minerals.* In L. Bragg, (Ed), The crystalline state. **4**. London: Bell and Sons.

Brunauer, S., Deming, L., Deming, W. and Teller, E.J. 1940. On a theory of the van der waals adsorption of gases. Journal American Chemical Society. **62**:1723-1732.

Burda, C., Chen, X. and Narayanan, R. 2005. Chemistry and properties of nanocrystals of different shapes. *Chemistry Reviews*. **105:** 1025-1102.

Carneiro, J.O., Teixeira, V., Portinha, A., Dupak, L., Magalhaes, A. and Coutinho, P. 2005. Study of the deposition parameters and Fe-dopant effect in the photocatalytic activity of TiO_2 films prepared by reactive magnetron sputtering. *Vacuum*. **78:** 37-46.

Chemseddine, A. and Moritz, T. 1999. Nanostructuring Titania: Control over nanocrystal structure size, shape and organization. *European Journal of Inorganic Chemistry*. **2:** 235-245

Chen, Y.F., Lee, C.Y., Yeng, M.Y. and Chiu, H.T. 2003. The effect of calcinations temperature on the crystallinity of TiO_2 nanopowders. *Journal of Crystal Growth*. **247**: 363-370.

Dongliang, H., Xiangju, M., Yanchun, T., Lin Z. and Fengshou, X. 2009. Synthesis of carbon doped TiO_2 using porous resin and its excellent photocatalytic properties . *Chinese Journal of Catalysis*. **30**(2): 83-85.

Eriksson, S., Nylen, U., Rojas, S. and Boutonnet, M. 2004. Preparation of catalysts from microemulsions and their applications in heterogenous catalysis. *Applied catalysis A: General*. **265**: 207-219.

Erkan, A., Bakir, U. and Karakas, G. 2006. Photocatalytic microbial inactivation over Pd doped SnO_2 and TiO_2 thin films. *Journal of Photochemistry and Photobiology A: Chemistry* **184:** 313-321.

Fisher, G.L., Hooper, A.E., Opila, R.L., Allara, D.L and Winograd, N. 2000. The Interaction of Vapor-Deposited Al Atoms with CO_2H Groups at the Surface of a Self-Assembled Alkanethiolate Monolayer on Gold. *Journal of Physical Chemistry B.* **104**: 3267-3327.

Frank, S.N. and Bard, A.J. 1977. Heterogeneous photocatalytic oxidation of cyanide ion in aqueous solutions at titanium dioxide powder. *Journal American Chemical Society*. **99:** 303-304.

Fujishima, A. and Honda, K. 1972. Electrochemical Photolysis of Water at a Semiconductor Electrode. *Nature*. **238**: 37-38.

Fujishima, A., Rao, T.N., Tryk, D.A. 2000. Titanium dioxide photocatalysis. *Journal of photochemistry and photobiology C: Photochemistry Reviews*. **1**: 1-21.

Gang, L., Lianzhou, W., Hua, G.Y., Hui-Ming, C. and Gao, L. 2010. Titania based photocatalyts;crystal growth, doping and heterostructuring. *Journal of Materials Chemistry*. **20**:831-843

Gao, B., Chen, G.Z. and Puma G.L. 2009. Carbon nanotubes/titanium dioxide ($CNTs/TiO_2$) nanocomposites prepared by conventional and novel surfactant wrapping sol gel methods exhibiting enhanced photocatalytic activity . *Applied Catalysis B: Environmental*. **89:** 503-509.

Goodboy, K.P. and Downing, J.C. 1990. *Production, Processes, Properties and Applications of Activated and Catalytic Aluminas*. Alumina Chemicals: Science and Technology Handbook E. 93-108

Guan, K. 2005. Relationship between photocatalytic activity, hydrophilicity and self-cleaning effect of TiO_2/SiO_2 films. *Surface Coating Technology*. **191**: 155-160.

Hart, L.D. 1990. *Alumina Chemicals: Sciences and Technology handbook.* Massmann Germany: Wiley.

Hart, L.D. and Lense, E. 1990. *Alumina Chemical. Science and Technology Handbook.* Nesterville, Ohio: American Ceramic Society.

Hashimoto, K., Irie H. and Fujishima, A. 2005. TiO_2 Photocatalysis: A historical overview and future prospects. *Japanese Journal of Applied Physics*. **44**: 8269-8285.

Hoffmann, M.R., Martin, S.T., Choi W. and Bahnemann D.W. 1995. Environmental Applications of Semiconductor Photocatalysis. *Chemical Review.* **95**: 69-96.

Hsiang, T. I., Wanchem, C. and Jeffrey, C.S.W. 2002. Photoreduction of CO_2 using sol–gel derived titania and titania-supported copper catalysts. *Applied Catalysis B: Environmental*. **37:** 37–48.

Hsiang, T.I. and Jeffrey, C.S.W. 2004. Chemical states of metal-loaded titania in the photoreduction of CO_2. *Catalysis Today.* **97:**113–119.

IEA, *World Energy Outlook 2010* (Paris: 2010),620.

Inagaki, M., Nakazawa, Y., Hirano, M., Kobayashi, Y. and Toyoda, M. 2001. Preparation of stable anatase-type TiO_2 and its photocatalytic performance, *International Journal of Inorganic Materials*. **3:** 809-811.

IPCC (2007), Revised 1996 IPCC Guidelines for National Greenhouse Gas Inventories (1996 IPCC Guidelines), IPCC, Bracknell, United Kingdom.

Joo, J., Kwon, S.G., Yu, T.Y., Cho, M., Yoon, J. And Hyeon, T. 2005. Large scale synthesis of TiO_2 nanorods via nonhydrolytic sol gel ester elimination reaction and their application to photocatalytic inactivation of E.coli. *Journal of Physical Chemistry B*. **109:** 15297-15302.

Jun, Y., Yung, Y. and Cheon J. 2002. Architectual Control of Magnetic Semiconductor Nanocrystals. *Journal of the American Chemical Society*. **14**: 615-619.

Karditsas, P.J and Baptiste, M.J (n.d). Thermal and Structural Properties of Fusion related Materials (online). http://www.ferp.ucsd.edu/LIB/PROPS/PANOS /al_2O_3.html (26^{th} February 2011)

Katsumi, K. 1994. Determination of pore size and pore size distribution adsorbents and catalyst. *Journal of Membrane Science*. **96**: 59-89.

Kim, C.S., Okuyama, K., Nakaso, K. and Shimada, M. 2004. Direct measurement of nucleation and growth modes in titania nanoparticles generation by a CVD methods. *Journal of Chemical Engineering of Japan*. **37**: 1379-1389.

Kobayashi, M., Tomita, K., Petrykin, V., Yoshimura, M. and Kakihana, M. 2007. Direct synthesis of brookite-type titanium oxide by hydrothermal method using water-soluble titanium complexe, *Journal of materials science*. **43**: 2158-2162

Kominami, H., Ishii, Y., Kohno, M., Konishi, S., Kera, Y. and Ohtani, B. 2003. Nanocrystalline brookite-type titanium(IV) oxide photocatalysts prepared by a solvothermal method: Correlation between their physical properties and photocatalytic activities. *Catalysis letters*. **91**: 41-47.

Kominami, H., Kato, J.I. and Murakami, S.Y. 2003. Solvothermal synthesis of semiconductor photocatalysts of ultra-high activities. *Catalysis Today*. **84:** 181-189.

Korosi, L. and Dekany, I. 2006. Preparation and investigation of structural and photocatalytic properties of phosphate modified titanium dioxide. *Colloids and Surface A*. **280:** 146-154.

Kumar, K.N.P., Keizer, K., Burggraaf, A.J., Okubo, T., Nagamoto, H. and Morooka, S. 1992**.** Densification of nanostructured titania assisted by a phase transformation . *Physical Chemistry Papers*. **358**: 48-51.

Lee, M.S., Hong, S.S. and Mohseni, M. 2005. Synthesis of photocatalytic nanosized TiO_2-Ag particles with sol-gel method using reduction agent. *Journal Molecular Catalysts A*. **242:** 135-140.

Lettmann, C., Hildebrand, K., Kisch, H., Macyk, W. and Maier, W. 2001. Visible light photodegradation of 4-chlorophenol with a coke-containing titanium dioxide photocatalyst. *Applied Catalysis B.* **32:** 215-227.

Li, B., Wang, X., Yan, M. and Li, L. 2002. Preparation and characterization of nano-TiO_2 powder. *Materials Chemistry and Physics*. **78**: 184-188.

Li, G.H., Yang, L., Jin, Y.X. and Zhang, L.D. 2000. Structural and optical properties of TiO_2 thin film and TiO_2 + 2 wt % $ZnFe_2O_4$ composite film prepared by radio frequency sputtering. *Thin Solid Films*. **368**: 163-167.

Li, X.H., Liu, W.M. and Li, H.L. 2005. Template synthesis of well aligned titanium dioxide nanotubes. *Applied Physics A: Materials Science and Processing*. **80**(2): 317-320

Li, X.Z. and Li, F.B. 2001. Study of Au/Au^{3+}-TiO_2 photocatalysts towards visible photooxidation for water and wastewater treatment. *Environmental Science Technology*. **35:** 2381-2387.

Li, X.Z. and Li, F.B. 2002. The enhancement of photodegradation efficiency using Pt-TiO_2 catalyst. *Chemosphere*. **48**: 1103-1111.

Li, Y., Li, X., Li, J. and Yin, J. 2006. Photocatalytic degradation of methyl orange by TiO_2 coated activated carbon and kinetic study. *Water Research*. **40**: 1119-1126.

Lopez, T., Sanchez, E., Bosch, P.,Means, P., and Gomez, M. 1992. FTIR and UV-Vis (diffuse reflectance) spectroscopic characterization of TiO, sol-gel. *Material Chemistry and Physics*. **32:**141-152.

Lowell, S. and Shields, J.E. 1998. Powder surface area and porosity (particle technology series). London, United Kingdom: Springer.

Lusvardi, V.S., Barteau, M.A., Chen, J.G., Eng, J., Fruhberger, B. and Teplyakov, A. 1998. An NEXAFS investigation of the reduction and reoxidation of TiO_2 (001). *Surface Science,* **397** (1-3):237-250.

Mandzy, N., Grulke, E. and Druffel, T. 2005. Breakage of TiO_2 agglomerates in electrostatically stabilized aqueous dispersions. *Powder Technology*. **160**: 121-126.

Manna, L., Scher, E.C. and Alivisatos, A.P. 2002. Shape control of colloidal semiconductor nanoctystal. *Journal of Cluster Science*. **13**: 521-532.

Mao, Y., Schoneich, C. and Asmus, K.D. 1991. Identification of organic acids and other intermediates in oxidatives degradation of chlorinated ethanes on titania surfaces route to mineralization: a combined photocatalytic and radiation chemical study. *Journal of Physical Chemistry*. **95**: 80-89.

Marius, S. and Gabriel, L. 2007. Application of Titanium Dioxide photocatalysis to create self-cleaning materials. *Romanian Technical Science Academy*. **3**: 280-285.

McZura, G., Goodboy K.P. and Koenig, J.T. 1978. *Aluminum Oxide. In: Kirk-Othmer Encyclopedia of Chemical Technology*, 3rd Edition. **2**. NewYork.

Mills, A., Elliott, N., Parkin ,I.P., O'Neil, S.A., and Clark, R.J. 2002. Novel TiO_2 CVD films for semiconductor photocatalysis. *Journal of Photochemistry and Photobiology*. **151**: 171-179.

Mills, A., Morris, S. and Davies, R. 1993. Shape control of colloidal semiconductor nanocrystals. *Journal of Photochemistry and Photobiology A: Chemistry.* **70:** 183-191.

Miyake, Y. and Kondo, T. 2001. Mesoporous Titania Prepared in the Presence of Alkylamine. *Journal of Chemical Engineering Japan*. **34**(3): 319-325.

Miyauchi, M., Ikezawa, A., Hashimoto, K. 2004. Zeta potential and photocatalytic activity of nitrogen doped TiO_2 thin films. *Physical Chemistry Chemical Physics.* **6:** 865-870.

Mo, J., Zhang, Xu, Q. and Yang, R. 2009. Effect of TiO_2/adsorbent hybrid photocatalysts for toluene decomposition in gas phase. *Journal of Hazardous Material*. **168:** 276-281.

Molino, F., Barthez, J.M. and Marignan, J. 1996. Influence on surfactants on the structure of titanium oxide gels: Experiments and simulations. *Physical Review E*. **53**: 921-925.

Morten, E., Simonsen, Erik, G., and Sogaard, J. 2010. Sol–gel reactions of titanium alkoxides and water: influence of pH and alkoxy group on cluster formation and properties of the resulting products. *Science Technology.* **53**: 485–497.

Murray, C.B., Kagan, C.R., Bawendi, M.G. 2000. Synthesis and Characterization of monodisperse nanocyrstals and close packed nanocrytal assemblies. *Annual Review of Material Science*. **30**: 545-610.

Nagaveni, K., Hedge, M.S., Ravishankar, N., Subbanna, G.N. and Giridhar, M. 2004. Synthesis and Structure of Nanocrystalline TiO_2 with Lower Band Gap Showing High Photocatalytic Activity. *Langmuir.* **20**: 2900-2907.

Nakajima, A., Fujishima, A., Hashimoto, K. and Watanabe T. 1999. Preparation of transparent superhydrophobic boehmite and silica films by sublimation of aluminium acetylacetonate. *Advanced Materials*. **11**: 1365-1368.

Nakajima, A., Koizumi, S. I., Watanabe, T. and Hashimoto, K. 2001. Effect of repeated photo-illumination on the wettability conversion of titanium dioxide. *Journal of Photochemistry and Photobiology A: Chemistry*. **146**: 129-132.

Nakaso, K., Okuyama, K., Shimada, M. and Pratsinis, S.E. 2003. Effect of reaction temperature on CVD-made TiO_2 primary particle diameter. *Chemical Engineering Science*, **58:** 3327-3335.

Navio, J.A., Testa, J.J., Djedjeian, P., Padron, J.R., Rodriguez, D. and Litter, M.I. 1999. Iron-doped titania powders prepared by a sol gel method, Part II: Photocatalytic properties. *Applied Catalysis A*: general, **178**: 191-203.

Nishimura, A., Mitsui, G., Hirota, M. and Hu, E. 2010. CO_2 reforming performance and visible light responsibility of Cr-doped TiO_2 prepared by sol-gel and dip coating method, *International Journal of Chemical Engineering*. **2010**

Oberlander, R.K. 1984. Aluminas for Catalysts: Their Preparation and Properties. In: Leach, B.E. *Applied Industrial Catalysis*. **3**: 63-112.

Ois, N.F. and Ginzberg, B. 1998. Parameters involved in the sol gel transition of titania in reverse micelles. *Journal of Sol Gel Science and Technology*. **13:** 341-346.

Panayiotis J.K. and Marc-Jean, B (1995). *Thermal and structural properties of fusion related materials*. (online) http://www- ferp.ucsd. edu/LIB/PROPS/PANOS /matintro.html (17^{th} February 2011)

Paola, A.D., Garcia-Lopez, E., Marci, G., Martin, C., Palmisano, L., Rives, V. and Venezia, A. 2004. Surface characterisation of metal ions loaded TiO_2 photocatalysts: structure-activity relationship. *Applied Catalysis B: Environment*. **48:** 223-233.

Pedro, K., Kiyohara, K., Helena, S.S., Antonio, C., Vieiera, C. and Persio, D.S.S. 2000. Structure, Surface Area and Morphology of Aluminas from thermal decomposition of $Al(OH)(CH_3COO)_2$ Crystals. *An Academia Brasileira de Ciências*. **72**(4): 471-495

Petlicki, J. and Van de Ven T.G.M., 1998. The equilibrium between the oxidation of hydrogen peroxide by oxygen and the dismutation of peroxyl or superoxide radicals in aqueous solutions in contact with oxygen**.** *Journal of the Chemical Society, Faraday Transactions*. **94**: 2763-2767.

Qiu, S. 2006. *Synthesis, processing and characterization of nanocrystalline TiO_2*. Master Thesis. University of Central Florida Orlando, Florida.

Rattan, L. 2004. Soil Carbon Sequestration Impacts on Global Climate Change and Food Security. *Science Journal*. **304**:623–27.

Sanchez, E. and Lopez, T. 1995. Effect of the preparation method on the band gap of titania and platinum-titania sol-gel materials. *Materials Letters*. **25**: 27 l-275

Saponjic, Z.V., Tiede, D.M. and Barnard, A.S. 2005. Shaping nanometers-scale architecture through surface chemistry. *Advanced Materials.* **17**: 965-971.

Sherill, A., Barteau, M.A. and Chen, J.G.G. 2000. Abstracts of papers of the American Chemical Society, 219: U532-U532.

Sherill, A., Medlin, J.W., Chen, J.G. and Barteau, M.A. 2001. NEXAFS investigations of cyclooctatetraene on TiO_2 (001). *Surface Science*. **492**(3):203-213.

Siti, A.I., and Srimala, S. 2010. Effect of pH on TiO_2 nanoparticles via sol gel method. International Conference on X-Rays & Related Techniques in Research and Industry. *Journal Advanced Materials Research*. **173**: 184-189.

Sivakumar, S., Sibu, C.P., Mukundan, P., Pillai, P.K. and Warrier K.G.K. 2004 . Nanoporous titania-alumina mixed oxides an alkoxide free sol gel synthesis. *Materials Letters*. **58:** 2664-2669.

Slamet, Nasution, H.W., Purnama, E., Kosela, S. and Gunlazuardi, J. 2005. Photocatalytic reduction of CO_2 on copper-doped titania catalysts prepared by improved impregnation method. *Catalysis Communication.* **6**: 313-319.

Soria, J., Conesa, J.C., Augugliaro, V., Palmisano, L., Schiavello M. and Sclafani A. 1991. Dinitrogen photoreduction to ammonia over titanium dioxide powders doped with ferric. *Journal of Physical Chemistry*. **95**(1): 274-282.

Stanford, U., Gray, K.A. and Kamat, P.V. 1993. An in situ diffuse reflectance on FTIR investigation of photocatalytic degradation of 4-chlorophenol on a TiO_2 powder surface. *Chemical Physics Letters*. **205**(1): 55-61.

Sung, S. C. 2004. Titania doped silica fibers prepared by electrospinning and sol gel process. *Journal of sol gel science and technology*. **30**: 215-221.

Swihart, M.T., 2003. Vapor-phase synthesis of nanoparticles. *Current Opinion in Colloid and Interface Science*. **8**: 127-133.

Takeshita, K., Yamakata, A., Ishibashi, T., Onishu, H., Nishijima, K. and Ohno, T. 2006. Transient IR absorption study of charge carriers photogenerated in sulfur-doped TiO_2. *Journal Photochemical and Photobiology*. **177**: 269-275.

Tian-Hua, X., Chen-Lu, S., Yong, L. and Gao-Rong, H. 2006. Band structures of TiO_2 doped with N, C and B. Journal of Zhejiang University Science B. **7**(4): 299-303.

Tonejc, M., Djerdj, I. and Tonejc, A. 2001. Evidence from HRTEM image processing, XRD and EDS on nanocrystalline iron-doped titanium oxide powders. *Material Science and Engineering B*. **85:** 55-63.

Treschev, S.Y., Chou, P.W., Tseng, T.H., Wang, J.B., Perevedentseva, E.V. and Cheng, C.L. 2008. Photoactivities of the visible light-activated mixedphase carbon-containing titanium dioxide: The effect of carbon incorporation. *Applied Catalysis B*. **79:** 8-16.

Uekawa, N., Kajiwara, J., Kakegawa, K. and Sasaki, Y. 2002. Low temperature synthesis and characterization of porous anatase TiO_2 nanoparticles. *Journal of Colloid and Interface Science*. **250:** 285-290.

Vijayan, B.K., Dimitrijevic, N.M., Wu, J., and Gray, K.A. 2010. The effects of Pt-doping on the structure and visible light photoactivity of titania nanotubes. *Journal Physical Chemistry*. **114**: 21262-212269.

Wang, Y.Q., Hu, G.Q. and Duan, X.F. 2002. Microstructure and formation mechanism of titanium dioxide nanotubes. *Chemical Physics Letters.* **365**: 427-431.

Wan-Jian, Y., Shiyou, C., Ji-Hiu, Y., Xin-Gao, G., Yanfa, Y. and Su-Huai, Wei. 2010. Effective band gap narrowing of anatase TiO_2 by strain along a soft crystal direction. *Applied Physics Letters*. **96**: 221901

Wei, M., Konishi, Y. and Zhou, H. 2005. Formation of nanotubes TiO_2 from layered titanate particles by a soft chemical process. *Solid State Communications*. **133**: 493-497.

Wu, J.C.S. and Chen, C.H. 2004. A visible-light response vanadium-doped titania nanocatalyst by sol-gel method. *Journal Photochemistry and Photobiology A*. **163**: 509-515.

Wu, J.C.S. and Chih-Yang, Y. 2001. Sol-gel Derived Photosensitive TiO_2 and Cu/TiO_2 Using Homogeneous Hydrolysis Technique. *Journal of Materials Research*. **16**(2): 615-620

Wu, M., Lin G., Chen D., Wang, G., He, D., Feng, S. and Xu, R. 2002 . Sol-hydrothermal synthesis and hydrothermally structural evolution of nanocrystal titanium dioxide. *Chemistry of Materials*. **14:** 1974-1980.

Wu, Z., Dong, F., Zhao, W. and Guo, S. 2008. Visible light induced electron transfer process over nitrogen doped TiO_2 nanocrystals prepared by oxidation of titanium nitride. *Journal of Hazardous Materials*. **157**(1): 57-63.

Xu, X., Zhang, J. and Song, G. 2003. Effect of complexation on the zeta potential of titanium dioxide dispersion. *Journal of Dispersion Science and Technology*. **24**: 527-535.

Yang, P., Lu, C., Hua, N. and Du, Y. 2002. Titanium dioxide nanoparticles Co-doped with Fe^{3+} and Eu^{3+} ions for photocatalysis. *Material Letters*. **57**: 794-801.

Yu, J., Zhou, M., Cheng, B. and Zhao, X. 2006. Preparation, characterization and photocatalytic activity of in situ N,S-codoped TiO_2 powders. *Journal of Molecular Catalysis A:* **246:** 176-184.

Zaleska, A., Sobczak J.W., Grabowska, E. and Hupka, J. 2007. Preparation and photocatalytic activity of boron-modified TiO_2 under UV and visible light. *Applied Catalysis B*. **78:** 92-100.

Zhang, Y., Ebbinghaus, S.G., Weidenkaff, A., Kurz, T., Von N.A.K., Klar, P.J., Gungerich, M. and Rellert, A. 2003. Controlled iron-doping of macrotextured nanocyrstalline titania. *Chemistry of Materials*. **15**(21): 4028-4033.

Zhu, H.Y., Lan, Y., Gao, X.P., Ringer, S.P. and Zheng, Z.F. 2005. Phase transition between nanostructures of titanate and titanium dioxides via simple wet-chemical reactions. *Journal of the American Chemical Society*. **127**: 6730-6736.

Zhu, J., Sheng, Q., Zheng, W., He, B., Zhang, J. and Masakazu, A. 2004. Characterization and photocatalytic reactivity of Fe-TiO_2 photocatalysts synthesized by hydrothermal method and their photocatalytic reactivity for photodegradation of XRG dye diluted in water. *Journal of Molecular Catalysis A: Chemical*. **216**: 35-43

Zhu, J., Zheng, W., He, B., Zhang, J. and Anpo, M. 2004. Characterization of Fe-TiO_2 photocatalysts sythesized by hydrothermal method and their photocatalytic reactivity for photodegradation of XRG dye diluted in water. *Journal of molecular catalysis A: Chemical*. **216**: 35-43.